MOLECULAR AND CELLULAR BIOLOGY, Sept. 1997, p. 4933–4947 Vol. 17, No. 9
0270-7306/97/$04.00+0

The Murine *Sim-2* Gene Product Inhibits Transcription by Active Repression and Functional Interference

PETER MOFFETT,[1] MARK REECE,[1] AND JERRY PELLETIER[1,2]*

Department of Biochemistry[1] and Department of Oncology,[2] McGill University, Montreal, Quebec, Canada H3G 1Y6

Received 21 January 1997/Returned for modification 14 March 1997/Accepted 2 June 1997

The *Drosophila single-minded* (*Dsim*) gene encodes a master regulatory protein involved in cell fate determination during midline development. This protein is a member of a rapidly expanding family of gene products possessing basic helix-loop-helix (bHLH) and hydrophobic PAS (designated a conserved region among PER, ARNT [aryl hydrocarbon receptor nuclear translocator] and SIM) protein association domains. Members of this family function as central transcriptional regulators in cellular differentiation and in the response to environmental stimuli such as xenobiotics and hypoxia. We have previously identified a murine member of this family, called *mSim-2*, showing sequence homology to the bHLH and PAS domains of Dsim. Immunoprecipitation experiments with recombinant proteins indicate that mSIM-2 associates with the arnt gene product. In the present work, by using fine-structure mapping we found that the HLH and PAS motifs of both proteins are required for optimal association. Forced expression of GAL4/mSIM-2 fusion constructs in mammalian cells demonstrated the presence of two separable repression domains within the carboxy terminus of mSIM-2. We found that mSIM-2 is capable of repressing ARNT-mediated transcriptional activation in a mammalian two-hybrid system. This effect (i) is dependent on the ability of mSIM-2 and ARNT to heterodimerize, (ii) is dependent on the presence of the mSIM-2 carboxy-terminal repression domain, and (iii) is not specific to the ARNT activation domain. These results suggest that mSIM-2 repression activity can dominantly override the activation potential of adjacent transcription factors. We also demonstrated that mSIM-2 can functionally interfere with hypoxia-inducible factor 1α (HIF-1α)/ARNT transcription complexes, providing a second mechanism by which mSIM-2 may inhibit transcription.

The basic helix-loop-helix PAS (Per-Arnt-Sim) (bHLH-PAS) protein family is a class of transcription factors with members present in vertebrates and invertebrates. These proteins contain a bHLH domain, a motif found in many transcription factors which undergo dimerization for function (for a review, see reference 42). The bHLH motif is present near the amino terminus of the protein and is contiguous with a second dimerization domain known as the PAS domain. The PAS domain, designated a conserved region among PER, ARNT (aryl hydrocarbon receptor nuclear translocator), and SIM, shows amino acid similarity over a stretch of 250 to 300 amino acids and contains degenerate hydrophobic repeats of approximately 50 amino acids each. Members of the bHLH-PAS protein family include (i) both subunits of the dioxin receptor complex, AHR (aryl hydrocarbon receptor) and ARNT, involved in the inducible expression of the *CYP1A1* gene by xenobiotics (5, 14, 26); (ii) a close homolog of ARNT, called ARNT-2, which has similar protein association and DNA binding properties to ARNT (12, 16, 25); (iii) hypoxia-inducible factor 1α (Hif-1α), a *trans*-acting factor that, as a dimer with ARNT, mediates the genetic response to low oxygen tension (31, 56); (iv) the *Drosophila trachealess* (*trh*) gene product required for embryonic tubulogenesis (29, 58); (v) the steroid receptor coactivators SRC-1 (61) and TIF2 (55); (vi) endothelial PAS protein 1 (EPAS1), a transcription factor that is expressed in endothelial cells and has properties similar to Hif-1α (54); (vii) the products of two genes expressed solely in the nervous system, NPAS1 and NPAS2 (62); (viii) the *single-minded* (*sim*) gene product, originally identified in *Drosophila* as being essential for midline development (9, 44, 53); and (ix) the *Drosophila similar* (*sima*) gene product, which is structurally related to Hif-1α and the *sim* gene product (43). Recently, Hogenesch et al. (27) reported on the cloning of five members of the PAS superfamily, which they term MOP1 to MOP5. Sequence analysis indicates that MOP1 corresponds to Hif-1α, MOP2 corresponds to EPAS1, MOP4 corresponds to NPAS2, and MOP5 corresponds to EPAS1, whereas MOP-3 is unique. The *Drosophila period* (*per*) and the prokaryotic *KinA* gene products contain PAS motifs but lack bHLH domains (28, 56).

Several groups have reported on the cloning of murine proteins showing high sequence homology to the bHLH and PAS domains of the *Drosophila sim* (*DSim*) gene product. The genes encoding these products have been designated *mSim* (15, 41, 60), *mSim-1*, (16, 17), and *mSim-2* (17). Sequence analysis indicates that *mSim* and *mSim-2* encode the same gene product. The bHLH-PAS regions of mSIM-1, mSIM-2, and DSIM show a high degree of similarity to each other, whereas there is little apparent conservation among the carboxy termini of these three proteins. Elucidating the conserved functional properties of these proteins will depend on defining their biochemical activities and identifying downstream targets.

It has been postulated that PAS-containing proteins can be divided into at least three classes (27, 40): (i) the ARNT group, which form both homo- and heterodimers; (ii) the SIM/AHR/HIF-1α group, which do not form homodimers but complex with HSP90 and then heterodimerize with members of the ARNT group (reference 40 and references therein); and (iii) PAS proteins, including SRC-1, PER, TIF2, and KinA, whose behavior does not fit well into the above two groups. ARNT can interact with a number of polypeptides of the second group, including AHR (23), HIF-1α (56), DSIM (15, 40, 51, 52), EPAS1 (54), mSIM-1 (16), and mSIM-2 (15, 16; see be-

* Corresponding author. Mailing address: McIntyre Medical Sciences Building, Rm. 902, 3655 Drummond St., McGill University, Montreal, Quebec, CANADA H3G 1Y6. Phone: (514) 398-2323. Fax: (514) 398-7384. E-mail: Jerry@Medcor.McGill.CA.

low). Although the above classification is useful in terms of predicting the behavior of some bHLH-PAS proteins, several members have properties which make their classification into a distinct group difficult. For example, Hogenesch et al. (27) have shown that MOP3, which appears to be related to ARNT based on sequence homology and on the fact that it can conditionally bind to AHR, also associates with HSP90. Also, the EPAS1/MOP2 polypeptide can interact with ARNT, but unlike most members of the second group, it does not seem to associate with HSP90 (27).

The activities of the mSIM, AHR, and HIF-1α proteins appear to be regulated at the transcriptional and posttranscriptional levels. Expression of *mSim-1* and *mSim-2* is spatially and developmentally restricted (16, 17, 41, 60); Hif-1α is active only in hypoxic cells (34, 56), and AHR, although present in a large variety of tissues and cell types (2, 6), dimerizes with ARNT only upon exposure to ligand (11, 26, 48). It appears that ARNT can act as a general dimerization partner for bHLH-PAS proteins of the second class, conceivably establishing a competitive situation whereby binding to ARNT may be limiting for some bHLH-PAS proteins. Accordingly, the rodent *arnt* gene is expressed in a large number of tissues throughout development and adult life (1, 6). Evidence in support of this hypothesis has emerged from studies performed by Gradin et al. (21), who demonstrated that HIF-1α can functionally compete with AHR for recruitment of ARNT, resulting in interference with the dioxin signaling pathway. These studies suggest the possibility of a complex cross talk network among bHLH-PAS proteins, indicating that the stoichiometry and affinity of protein partners may be important in determining functional complex formation, which, in turn, will elicite an appropriate transcriptional response.

A number of mechanisms by which bHLH-PAS family members regulate transcription have been defined. ARNT, ARNT-2, AHR, and HIF-1α have transcriptional activation domains at their carboxy termini (25, 30, 31, 34, 38, 57), MOP2/EPAS1 has been shown to activate transcription as a heterodimer with ARNT (27, 54), and SRC-1 and TIF2 act as transcriptional coactivators (55, 61). The carboxy terminus of DSIM is a potent activator when fused to a heterologous DNA binding domain (18). Ema et al. (16) have shown that mSIM-1 and mSIM-2 can inhibit ARNT-mediated activation but did not define the intrinsic transcriptional properties of mSIM-2, the specificity of the response, the responsible mSIM domain(s), or the mechanism by which this inhibition was being achieved. In this study, we used fine-structure mapping to demonstrate that the HLH and PAS domains of mSIM-2 and mARNT are required for in vitro and in vivo interaction. We found that the carboxy terminus of mSIM-2 contains two independent transcription repression domains. We demonstrated that mSIM-2 can repress ARNT-mediated transcriptional activation in a mammalian two-hybrid system. This repression phenomenon requires an intact dimerization domain, as well as the mSIM-2 carboxy-terminal domain, and was not specific for the ARNT activation domain. We also demonstrated that mSIM-2 can functionally interfere with HIF-1α/ARNT-dependent activation under hypoxic conditions. These results define the structural requirements for the mSIM-2/ARNT interaction and demonstrate that mSIM-2 can repress transcription by two distinct mechanisms: direct repression and functional interference.

MATERIALS AND METHODS

Materials and general methods. Restriction endonucleases, calf intestinal alkaline phosphatase, the Klenow fragment of DNA polymerase I, T4 DNA ligase, and T4 DNA polymerase were purchased from New England Biolabs. [^{3}H]CTP (21.8 Ci/mmol) and [^{35}S]methionine (>1,000 Ci/mmol) were obtained from New England Nuclear. D-Threo-[dichloroacetyl-1-^{14}C]chloramphenicol (54.0 Ci/mmol) was purchased from Amersham. SP6 RNA polymerase was from Promega Biotec. T7 RNA polymerase and m^{7}GpppG was purchased from New England Biolabs. Human placental RNase inhibitor was from Pharmacia.

Preparation of plasmid DNA, restriction enzyme digestion, agarose gel electrophoresis of DNA, DNA ligation, and bacterial transformations were carried out by standard methods (reference 49 and references therein). Subclones of DNA PCR amplification products were always sequenced by the chain termination method (50) with double-stranded DNA templates to ensure the absence of unwanted secondary mutations.

Recombinant plasmids. Deletion constructs of mSIM-2 used for coimmunoprecipitation experiments (see Fig. 1A) were derived from pSP/ΔmSim, which lacks the *mSim-2* 5′ untranslated region and has a modified ATG initiation codon (41). The boundaries of the clones are defined by indicating the deleted (Δ) or remaining amino acids. To generate ΔbHLH, a partial cDNA clone of mSIM-2 (RPS3B [41]) was digested with *Bam*HI (which cleaves within the pKS II+ polylinker and at nucleotide (nt) +240 relative to the A residue of the *mSim-2* ATG codon). The vector containing the mSIM-2 PAS domain was repaired with the Klenow fragment of DNA polymerase I, gel purified, and ligated to *Nco*I linkers (5′ pCAGCC**ATG**GCTG 3′ [New England Biolabs]), thus introducing an in-frame initiation codon (shown in boldface type). The *Spe*I-*Bst*EII fragment of this clone was then transferred to pSP64 in a three-way ligation involving pSP64 linearized with *Xba*I and *Eco*RI and a *Bst*EII-*Eco*RI fragment containing the C terminus of mSIM-2 obtained from pSP/ΔmSim. ΔbH1 was derived by digesting pSK/2A (41) with *Not*I, followed by Klenow repair and digestion with *Xba*I. The fragment containing the N terminus of mSIM-2 was gel purified and ligated to ΔbHLH, which had been linearized with *Nco*I, subjected to Klenow repair, and digested with *Xba*I. To generate SIMC, ΔbHLH was digested with *Nco*I and *Eco*RI and ligated to the *Nco*I-*Eco*RI C-terminal SIM fragment obtained from pcDNA3/GAL4/SIMC (described below). Clone Δb was constructed by PCR-mediated mutagenesis with an upstream primer 5′ ATGGCC**ATG**GAGAAGGAAAATGGC 3′ (initiation codon in boldface type) and a primer downstream of the *Xba*I site (nt +260). The subsequent PCR product was digested with *Xba*I-*Nco*I and cloned into ΔbHLH. Clone ΔH2 was constructed by PCR-mediated mutagenesis with a primer (5′ CCACGCGTCTCCGTCCAGCTGCGAGGTG 3′) spanning an internal *Mlu*I site and primer s-ATG (41). The PCR product was digested with *Mlu*I and *Xho*I and cloned into the *Mlu*I-*Sal*I sites of pSP/ΔmSim. Clone SIML was constructed by PCR-mediated mutagenesis with a primer (5′ GACTCTAGATGG ATTTGTGTTCGACGTGGCCTCTGATGGC 3′) targeting the appropriate nucleotides (shown by an underline) and a primer downstream of the *Sac*I site (nt +351). The PCR product was digested with *Xba*I and *Sac*I and cloned into the same sites of pSP/ΔmSim. Constructs bHLHAB and bHLHA were generated by restriction enzyme digestion of pSP/ΔmSim with *Acc*I or *Bst*BI, respectively, followed by Klenow repair and ligation-recircularization with an *Xba*I linker (5′ pCTAGTCTAGACTAG 3′ [New England Biolabs]) containing stop codons in all three translation reading frames. Constructs ΔA and ΔAB were generated by removal of the appropriate regions by restriction digestion (*Mlu*I-*Bst*BI and *Xba*I-*Acc*I, respectively), repair of the ends with Klenow polymerase, and religation with T4 DNA ligase.

To construct a hemagglutinin (HA) epitope-tagged ARNT protein (HA-ARNT) for coimmunoprecipitation experiments, a *Not*I restriction site was introduced at the 5′ end of the ARNT cDNA by PCR with pcDNA/Neo/mARNT as a template and primers ATNOT (5′ GCGGCCGCACC**ATG**GCGG CGACTAC 3′) (the initiation codon is indicated in boldface type, and the *Not*I site is underlined) and ATAS1 (5′ TGGGAGAACTAGTTACC 3′). This PCR product was ligated into the *Eco*RV site of pKS II+ (Stratagene), and a clone was selected in which the 5′ end of ARNT was adjacent to the T3 promoter. We named this clone pKS/ATNOT. To construct pKS/ARNT, the ARNT cDNA was excised from pcDNAI/Neo/mARNT with *Nco*I and *Bam*HI and ligated into the *Nco*I and *Bam*HI sites of pKS/ATNOT. The *Not*I fragment from pKS/ARNT was subcloned in frame into pACTAG-2 (7), which contains a T7 promoter, a start codon followed by three consecutive HA epitope tags (YPYDVPDVASL), and a *Not*I cloning site, to create pACTAG-2/mARNT.

The generation of pcDNAI/Neo/mARNT and deletion mutants has been described previously (47) (see Fig. 2A). SIM-HA was generated by PCR-mediated mutagenesis with an oligonucleotide (5′ GATGAATTCACAGGGAGG CGTAGTCGGGGACGTCGTAGGGGTACCTGCCGTTGGTGATGATG 3′) which introduced an HA epitope tag immediately upstream of the mSIM-2 termination codon and an *Eco*RI site downstream of the stop codon.

For the yeast two-hybrid study, GAL4 activation domain (AD) constructs pACT II and pGAD 424, along with the GAL4 DNA binding domain (DBD) construct pGBT9 (Clontech), were used. Complementary DNAs for ARNT and ARNT(bHLHAB) were transferred from pcDNA1/Neo/mARNT into pACT II with the *Nco*I-*Bam*HI and *Nco*I-*Xho*I restriction sites, respectively. An *Eco*RI site was introduced at the 5′ end of the mSIM-2 cDNA by PCR-mediated mutagenesis to allow cloning of the complete coding sequence into the *Eco*RI sites of pGBT9 and pGAD 424. To construct mSIM-2 fusion proteins lacking the carboxy terminus, pGBT9/SIM was digested with *Acc*I, subjected to Klenow repair, digested with *Eco*RI, and transferred into the *Eco*RI-*Sma*I sites of pGAD 424 and pGBT9.

For *trans*-repression studies, *mSim-2* fusion derivatives containing the Gal4 DBD were generated (see Fig. 5A and 6A). A vector containing the GAL4 DBD in pcDNA3 was generated by ligating a PCR product, containing amino acids (aa) 1 to 92 of the GAL4 transcription factor, into the *Hin*dIII site of pcDNA3. This plasmid was named pcDNA3/GAL4(1–92). A separate expression vector, encoding the complete DBD of GAL4, was constructed by transferring the *Hin*dIII-*Dra*I fragment (which had been blunt ended with Klenow polymerase) of pGBT9 into pKS II+ which had been linearized with *Eco*RI-*Bam*HI and repaired with Klenow polymerase. The *Hin*dIII-*Xba*I fragment of the resultant clone was then transferred into the *Hin*dIII-*Xba*I sites of pcDNA3 to yield pcDNA3/GAL4(1–147). pcDNA3/GAL4/SIM was generated by transferring the *Hpa*I-*Eco*RI *mSim-2* fragment from the yeast two-hybrid shuttle vector, pGBT9/SIM, into pcDNA3/GAL4(1–92). The resultant construct encodes a fusion protein containing aa 1 to 147 of GAL4 and aa 1 to 657 of mSIM-2. Deletion derivatives of *mSim-2* were transferred from pSP64 (see Fig. 1) into either the *Nco*I and *Sma*I sites of the yeast two-hybrid shuttle plasmid, pASI (which contains the Gal4 DBD), followed by transfer into pcDNA3/GAL4/SIM with *Hpa*I and *Sac*II or directly into pcDNA3/GAL4/SIM. GAL4/ΔB was generated by digesting pcDNA3/GAL4/SIM with *Pfl*MI, repairing with T4 DNA polymerase, redigesting with *Pvu*II, and recircularizing with T4 DNA ligase. pcDNA3/GAL4/SIMC was constructed by transferring the *Acc*I (Klenow repaired)-*Eco*RI fragment of the *mSim-2* cDNA into pAS1, followed by transfer of the *Hpa*I-*Sac*II fragment into pcDNA3/GAL4/SIM which had been linearized with the same enzymes. GAL4/BC was constructed by first transferring the *Afl*III-*Sac*II fragment of the mSIM-2 cDNA into the *Nco*I-*Sac*II sites of pASI/SIMC. Subsequently, the *Hpa*I-*Sac*II fragment was subcloned into pcDNA3/GAL4/SIM. GAL4/SIM-PS and GAL4/SIM-PA were generated by PCR amplification of the cDNA corresponding to the amino acids indicated in Fig. 6A with primers to introduce an *Nco*I site upstream and a stop codon downstream of the targeted sequence. After digestion with *Nco*I, the fragments were inserted into the *Nco*I site of pASI. The GAL4/SIM moiety was then isolated by digestion with *Hpa*I and *Sal*I and transferred to the *Hpa*I and *Xho*I sites of pcDNA3/GAL4. GAL4/SIM-ST and GAL4/SIMST-PS (see Fig. 6A) were generated by PCR amplification with a ΔB *mSim-2* cDNA as template, with a primer upstream of the *mSim-2* *Afl*III site and a second primer to introduce a stop codon downstream of the targeted sequence. The PCR product was digested with *Afl*III and ligated into the *Nco*I site of pASI. The GAL4/SIM moiety was isolated by digestion with *Hpa*I and *Sal*I and transferred to the *Hpa*I and *Xho*I sites of pcDNA3/GAL4. To construct GAL4/SIM-PS-PA, the *Hpa*I-*Spe*I fragment of pASI/PS was transferred into the *Hpa*I and *Spe*I sites of pcDNA3/GAL4/SIMC. GAL4/SIM-PAΔS was constructed by digestion of GAL4/SIM-PA with *Sac*II followed by repair with T4 DNA polymerase and recircularization in the presence of an *Xba*I stop linker.

For the mammalian two-hybrid system, pASI/ARNT and pASI/ARNT bHLHAB were generated by transferring the *Nco*I-*Xho*I fragments from pcDNAI/Neo/ARNT derivatives into pASI. pcDNA3/GAL4/ARNT and pcDNA3/GAL4/ARNTbHLHAB were constructed by transferring the *Xho*I fragments from the corresponding pASI/ARNT derivatives into pcDNA3/GAL4/SIM. Plasmids pcDNA3/SIM, pcDNA3/SIMbHLHAB, pcDNA3/SIMΔbHLH, and pcDNA3/SIMΔAB were generated by transferring the *Hin*dIII-*Eco*RI inserts from the corresponding pSP64 derivatives (see Fig. 1) into the *Hin*dIII and *Eco*RI sites of pcDNA3. pcDNA3/SIMΔB was obtained by transferring the *Xba*I fragment from pcDNA3/GAL4ΔB into pcDNA3/GAL4/SIM. To swap the ARNT AD for the GAL4 AD, the GAL4 AD was excised from pGAD 424 by restriction digestion with *Hin*dIII and ligated into the *Hin*dIII site of pKS and a clone was selected wherein the 5′ end of the *GAL4* open reading frame was oriented towards the T3 promoter. This generated pKS/GAL4 AD. This clone was digested with *Xba*I followed by partial digestion with *Kpn*I, generating a fragment wherein only the *Kpn*I site from the pKS polylinker was cleaved (but not the *Kpn*I site within the *GAL4* cDNA). To generate pcDNA3/GAL4/ARNT/GAL4, this fragment was gel purified and used in a triple ligation with pcDNA3/GAL4/ARNT which had been digested with *Xba*I and *Pfl*MI and the *Pfl*MI-*Kpn*I fragment of the ARNT cDNA. The resulting construct encodes a fusion protein of the GAL4 DBD(1–147), ARNT(1–516), and the GAL4 AD(769–882) as illustrated in Fig. 6A. To express HIF-1α in eukaryotic cells, pcDNA3/Hif-1α was generated by digesting pSK/Hif-1α (56) with *Ase*I followed by T4 DNA polymerase repair and digestion with *Kpn*I. This fragment was then ligated into the *Kpn*I and *Eco*RV sites of pcDNA3.

The reporter construct 5×Gal4/E1B/CAT contains five GAL4 DNA binding sites upstream of the minimal E1B promoter and has been described previously (35). Reporter constructs pTECAT and pTECAT/(5×Gal4) were constructed by inserting the *Hin*dIII-*Xho*I fragments of pBLCAT2 and 5×Gal4*tk*CAT (39), respectively, into the *Hin*dIII-*Sal*I sites of pCAT-ENHANCER (Promega Biotech). TK(2×Gal2)/CAT is essentially the same as pTECAT except that two GAL4 DNA binding sites have been inserted into the *Bgl*II site immediately downstream of the thymidine kinase (TK) promoter (nt −105 to +51), placing them in the 5′ untranslated region of the chloramphenicol acetyltransferase (CAT) gene.

In vitro dimerization. Derivatives of pcDNA1/Neo/mARNT and pSP/ΔmSIM were transcribed with T7 and SP6 RNA polymerase, respectively (as specified by the manufacturer). Transcriptions were performed in the presence of [^{3}H]CTP to allow for accurate quantitation of the transcripts. RNAs were transcribed in a rabbit reticulocyte lysate system, in the presence or absence of L-[^{35}S]methionine, at an RNA concentration of 20 μg/ml as specified by the manufacturer (Promega). The relative amounts of protein produced in each translation were determined by subjecting an aliquot of the [^{35}S]methionine-labeled reaction mixture to trichloroacetic acid precipitation. Coimmunoprecipitations were performed by incubating unlabeled HA-tagged proteins with ^{35}S-labeled untagged proteins at a molar ratio of 1:3 at room temperature for 1 h. At the end of this incubation period, 1 μg of purified 12CA5 antibody (anti-HA; Boehringer Mannheim) was used for immunoprecipitation (IP) of complexes in IP buffer (25 mM HEPES [pH 7.5], 1.2 mM EDTA, 200 mM KCl, 10% glycerol, 0.1% Nonidet P-40) at room temperature for 1 h. The antigen-antibody complexes were captured with protein G-Sepharose 4 Fast Flow beads (Pharmacia) for 1.5 h at room temperature. The pellets were washed three times with IP buffer and once with phosphate-buffered saline, and then boiled in sodium dodecyl sulfate (SDS) sample buffer (33). The IP products and corresponding supernatants were subjected to analysis by SDS-polyacrylamide gel electrophoresis (PAGE) on a 12% gel, which was subsequently treated with En^{3}HANCE (Du Pont), dried, and exposed to X-ray film (Kodak X-OMAT AR). Radioactivity was quantitated by phosphoimage scanning (Fujix BAS 2000).

Yeast two hybrid system. *Saccharomyces cerevisiae* HF7c was transformed with shuttle plasmids expressing the GAL4 AD or GAL4 DBD fused to full-length or carboxy-terminal truncated forms of mSIM and mARNT (see above). Transformants (two or three colonies) were incubated overnight in 10 ml of SD medium selective for leucine, tryptophan, and histidine and containing 15 mM 3-aminotriazole (Sigma). The overnight culture was diluted into YPD medium and incubated at 30°C until an optical density at 600 nm of 0.5 to 0.8 was obtained. The cells were collected by centrifugation and resuspended in 300 μl of Z-buffer (60 mM Na_2HPO_4, 40 mM NaH_2PO_4, 10 mM KCl, 1 mM $MgSO_4$), and duplicates of this cell suspension (100 μl) were lysed by rapid freezing in liquid nitrogen followed by thawing at 37°C. Then 700 μl of Z-buffer (containing 0.27% 2-mercaptoethanol) and 160 μl of *o*-nitrophenol-β-D-galactopyranoside (ONPG) (4 mg/ml in Z-buffer) were added, and the reaction mixtures were incubated at 37°C until a yellow color was discernible. The reaction was terminated by the addition of 400 μl of 1 M Na_2CO_3. Cell debris was removed by centrifugation for 10 min in a microcentrifuge, and the optical density at 420 nm was recorded. β-Galactosidase activity was expressed in units calculated as previously described (13).

Cell lines, transfections, and CAT assays. COS-7 cells were maintained in Dulbecco's modified Eagle's medium supplemented with 10% heat-inactivated fetal calf serum (Gibco BRL), penicillin, and streptomycin. For transient transfections, the cells were plated at a density of 2×10^5 to 5×10^5 cells per 100-mm dish 24 h prior to transfection. The cells were transfected by the calcium phosphate precipitation method (49). Individual DNA precipitates were adjusted to contain equal amounts of total DNA by the addition of the empty expression vector, pcDNA3. To normalize for transfection efficiency, cells were cotransfected with 2 μg of pRSV/β-gal or β-actin/β-gal. At 48 h after transfection, the cells were harvested and assayed for β-galactosidase and CAT activity (20). Following thin-layer chromatography analysis, regions containing acetylated [^{14}C]chloramphenicol, as well as unacetylated [^{14}C]chloramphenicol, were quantitated by direct analysis on a PhosphorImager (Fujix BAS 2000). All CAT activity values were normalized to β-galactosidase values, which served as internal controls for the transfections.

RESULTS

Association of mSIM-2 mutants with ARNT. The ARNT and mSIM-2 polypeptides can associate in vivo and in vitro (15, 16, 45). To define the domain(s) required for this interaction, we undertook a fine-structure analysis of both proteins. A series of mSIM-2 deletion mutants were constructed to identify domains necessary for ARNT association (Fig. 1A). These mutations specifically target (i) the bHLH domain (Δb, ΔbH1, ΔH2, and ΔbHLH), (ii) the PAS domains (ΔA and ΔAB), (iii) the carboxy-terminal portion of mSIM-2 (bHLHAB), and (iv) several domains in combination (bHLHA and SIMC). In addition, a missense alteration, modeled after the *Per^L* allele, was introduced into mSIM-2 (SIML). This mutation results in altered circadian rhythm in *Drosophila* and disrupts both homo- and heterodimerization properties of the PER protein (28).

To assess dimerization efficiency, full-length mSIM-2 and deletion derivatives were generated by in vitro transcription and translation. [^{35}S]methionine-labeled products were incubated with unlabeled ARNT protein containing three amino-terminal HA epitope tags (HA-ARNT). Following immunoprecipitations and SDS-PAGE analysis, the in vitro dimerization ef-

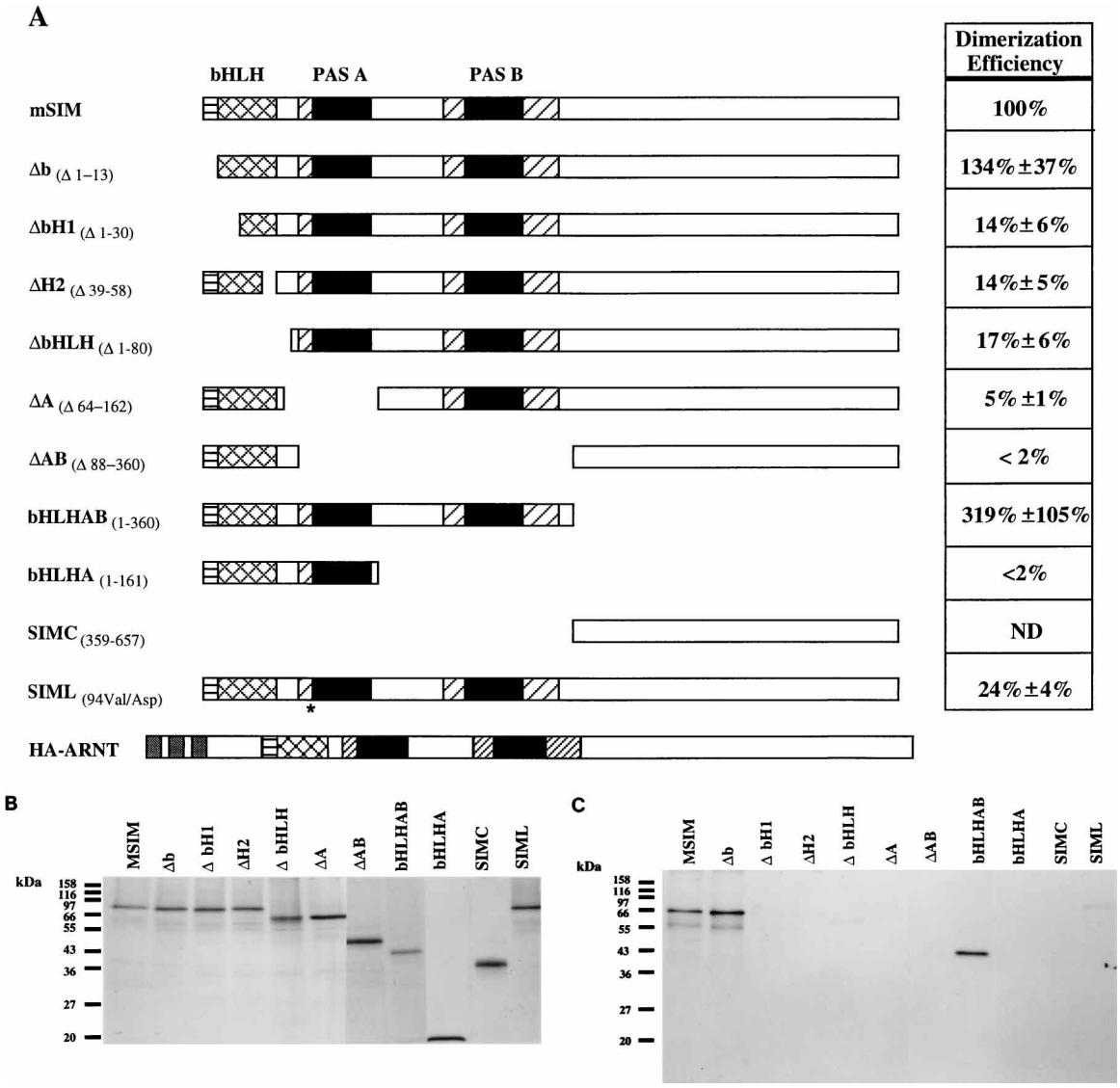

FIG. 1. Definition of the mSIM-2 domain required for ARNT association. (A) Schematic representation of mSIM-2 mutants used in this study. Boundaries defined by deleted or mutated amino acids are indicated in parentheses as subscripts to the name of each construct. Solid boxes represent the PAS A and PAS B direct repeats, and hatched areas flanking the repeats represent extended sequence similarity to the PER, AHR, and ARNT proteins. Cross-hatched boxes represent the HLH domain, and horizontally lined boxes represent the basic domain. The HA epitope tags present at the amino terminus of ARNT are represented by gray boxes, and the asterisk represents a missense mutation in mSIM-2 converting ^{94}Val to ^{94}Asp. Dimerization efficiency was calculated by assessing the percentage of immunoprecipitated protein, relative to IP of full-length mSIM-2 protein in the same experiment, which was set as 100%. The results represent the mean of at least four independent experiments. ND, not detectable. (B) Analysis of mSIM-2 translation products. Following in vitro transcription-translation of *mSim-2* and deletion mutants, protein yields were quantitated by trichloroacetic acid precipitation. Equimolar amounts of translation products were analyzed by SDS-PAGE (12% polyacrylamide) followed by fluorography and autoradiography. The relative molecular mass of protein standards (New England Biolabs; broad-range markers) are indicated to the left. (C) Analysis of mSIM-2 co-IP products with HA-ARNT. Prior to the IP, unlabeled HA-ARNT was incubated with the radiolabeled mSIM-2 products indicated at the top of each lane. The efficiency of HA-ARNT in vitro translations was monitored by performing parallel reactions in the presence of [^{35}S]methionine. Following co-IP, the proteins were analyzed by SDS-PAGE (12% polyacrylamide) and visualized by fluorography and autoradiography. Control co-IP reactions with unprogrammed reticulocyte lysate, in lieu of HA-ARNT, failed to precipitate mSIM-2 protein (41a). The relative molecular masses of protein standards (New England Biolabs) are indicated to the left.

ficiencies of the mSIM-2 deletion mutants were calculated from at least four independent experiments and are listed in Fig. 1A. A representative experiment is illustrated in Fig. 1B and C. Direct visualization of the mSIM-2 translation products revealed a single major protein species for all constructs assayed (Fig. 1B). Incubation of these mSIM-2 protein products with HA-ARNT, followed by immunoprecipitation, revealed that only a subset of these products associated efficiently with ARNT (Fig. 1C). The 12CA5 antibody routinely precipitated ~30 to 40% of HA-ARNT-tagged protein and showed no background precipitation of SIM proteins lacking an epitope tag (41a). Deletion of the mSIM-2 putative DNA binding basic region did not affect the efficiency of dimerization with HA-ARNT (Fig. 1C, compare Δb with MSIM). However, mSIM-2 deletions which removed the first helix (ΔbH1), the second helix (ΔH2), or the entire bHLH domain (ΔbHLH) associated weakly (14 to 17%) with HA-ARNT, compared to full-length mSIM-2 (Fig. 1C, compare ΔbH1, ΔH2, and ΔbHLH to

MSIM), indicating that both helices of the mSIM HLH motif are required for efficient dimerization. Deletion of PAS A (ΔA), PAS A and PAS B (ΔAB), or PAS B and the carboxy terminus (bHLHA) abolished HA-ARNT association (Fig. 1C, compare ΔA, ΔAB, and bHLHA to MSIM), implying that both hydrophobic repeats of the mSIM-2 PAS domain are necessary for heterodimerization. The carboxy-terminal half of mSIM-2, encoded by *simC*, showed no binding activity to HA-ARNT (Fig. 1C). On the other hand, deletion of only the carboxy terminus (bHLHAB), led to a small but reproducible increase in HA-ARNT association (ca. two- to threefold increase relative to wild-type mSIM-2) (Fig. 1C, compare bHLHAB to MSIM). These results demonstrate that the bHLH-PAS region of mSIM-2 is sufficient and necessary for dimerization with HA-ARNT. Our results illustrate that the domains used by mSIM-2 for ARNT association are similar to those of two other ARNT partners: AHR (19) and HIF-1α (31) (see Discussion).

We assessed the essential nature of the mSIM-2 PAS A domain for HA-ARNT association by introducing a missense mutation within this region (SIML), converting a conserved valine residue to an aspartic acid. We reasoned that since this mutation abolishes homo- and heterodimerization of the *Drosophila* PER protein, it may have the same effect on the dimerization potential of other PAS-containing proteins. As predicted, this mutation severely affected the ability of SIML to interact with HA-ARNT (Fig. 1C, compare SIML to MSIM), suggesting a conserved function for this amino acid in PAS protein dimerization.

Association of ARNT mutants with mSIM-2. To define the ARNT domain(s) required for mSIM-2 interaction, we tested a series of mutants previously employed to define the structural basis of ARNT/AHR heterodimerization (47). These mutations specifically targeted (i) subdomains of the ARNT bHLH region (Fig. 2A; Δb, ΔH1, ΔH2, ΔHLH, and ΔbHLH), (ii) the PAS domains (ΔA and ΔAB), (iii) the carboxy-terminal region (bHLHAB), and (iv) combinations of these regions (bHLHA and AB). For immunoprecipitation experiments, a full-length mSIM-2 construct containing an HA epitope tag at the carboxy terminus (SIM-HA) was used.

Full-length and deletion mutants of ARNT were generated by in vitro transcription-translation reactions. The integrity of the translation products was assessed by SDS-PAGE analysis (Fig. 2B). Following preincubation of the ARNT translation product with unlabelled SIM-HA, coimmunoprecipitation experiments were performed with the 12CA5 monoclonal anti-HA antibody. The average values for association efficiency, calculated from three separate experiments, are tabulated in Fig. 2A. A representative experiment is provided in Fig. 2B and 2C. Deletion of the ARNT DBD had no effect on mSIM-2–ARNT association (Fig. 2C, compare Δb to ARNT). However, in contrast to the results obtained with SIM ΔbH1 and HA-ARNT (Fig. 1C), ARNT ΔH1 bound to mSIM-2 with 66% efficiency relative to wild-type ARNT (Fig. 2C, compare ΔH1 to ARNT). Deletion of the second helix (ΔH2) or the entire HLH region (ΔHLH and ΔbHLH) significantly reduced the association efficiency with SIM-HA (Fig. 2C, compare ΔH2, ΔHLH, and ΔbHLH to ARNT), similar to results obtained with the corresponding mSIM-2 deletions and ARNT-HA (Fig. 1). Removal of either PAS A or PAS B (ΔA and bHLHA, respectively) significantly decreased the association efficiency with SIM-HA (Fig. 2C, compare ΔA and bHLHA to ARNT). Deletion of the entire PAS domain (ΔAB) had a drastic effect on the ability of the resultant mutant to associate with mSIM-2 (Fig. 2C, compare ΔAB to ARNT). A mutant lacking the ARNT carboxy terminus and the amino-terminal first 70 aa associated with SIM-HA at similar efficiencies to those of wild-type ARNT (Fig. 2C, compare bHLHAB to ARNT). The ARNT PAS domain was able to bind to mSIM-2 with ~48% efficiency relative to wild-type ARNT (Fig. 2C, compare AB to ARNT), whereas an ARNT deletion lacking the HLH region (ΔHLH) associated with only a 15% efficiency. It is possible that this indicates that the specified domains are not entirely modular in activity or, alternatively, that some of the deletion mutants studied are incorrectly folded. At present we cannot distinguish between these two possibilities. It has been reported that ARNT can form homodimers (3, 51). We have not observed such complexes under the specific in vitro conditions used in this study (data not shown), and Reisz-Porszasz et al. (47) have not observed them in a similar study. Therefore it is unlikely that the propensity of ARNT to homodimerize is influencing the heterodimer yields with mSIM-2 in our assay. Our results indicate that both the HLH and PAS domains of ARNT contribute to the overall efficiency of association with mSIM-2.

MSIM-2 does not self-associate. Previous studies of the *Drosophila Per* and mammalian *Arnt* gene products have indicated that these proteins can form homodimers (3, 16, 28, 51) and that this ability may form the basis for the division of bHLH-PAS proteins into distinct subgroups (27, 40). The ability of mSIM-2 to form homodimers has important implications for gene regulation, since this propensity could be a mechanism by which levels of mSIM-2/ARNT complexes are controlled. To address this issue, [^{35}S]methionine-labeled mSIM-2 was incubated with either mock-translated reticulocyte lysate (Fig. 3, lane 3) or a threefold molar excess of unlabeled SIM-HA (lane 2). IPs were performed with anti-HA antibodies. Whereas radiolabeled SIM-HA was efficiently immunoprecipitated by 12CA5 (lane 1), no radiolabeled mSIM-2 could be coprecipitated with unlabeled SIM-HA (lane 2). Analysis of the supernatant from this coIP reaction demonstrated that mSIM-2 protein was intact and was not associated with SIM-HA (lane 4). These results indicate that mSIM-2 does not self-associate efficiently under conditions used to assess mSIM-2/ARNT interactions. They do not rule out the possibility that mSIM-2 can homodimerize in vivo in specific situations (e.g., on DNA templates containing appropriate recognition motifs).

The bHLH-PAS domain is required for ARNT–mSIM-2 association in vivo. Ema et al. (16) and Probst et al. (45) have used the yeast two-hybrid system to demonstrated that mSIM-2 and ARNT can associate in vivo. We have taken advantage of this system to demonstrate several aspects of the mSIM-2/ARNT interaction (Table 1). Activation vectors expressing either full-length ARNT, or only the ARNT bHLH-PAS region, fused to the GAL4 AD were generated (Table 1, pACT II derivatives). In addition, full-length mSIM-2 or the mSIM-2 bHLH-PAS region was fused to the GAL4 DBD (Table 1, pGBT9 derivatives) and to the GAL4 AD (Table 1, pGAD derivatives). A summary of results obtained with combinations of DBD and AD expression vectors are presented in Table 1. The expression cassettes, pGAD and pACT II, produced very low β-galactosidase levels when introduced into our reporter yeast strain either alone or in combination with pGBT9/SIM or pGBT9/SIM(bHLHAB) (Table 1). Likewise, pACT II/ARNT or pGAD/SIM vectors in combination with pGBT9 produced very little β-galactosidase in this system (Table 1). However, a significant level of β-galactosidase activity was obtained when pGBT9/SIM was combined with pACT II/ARNT or pACT II/ARNT(bHLHAB). Even higher levels of β-galactosidase were observed when the bHLHAB region of mSIM-2 was present with either ARNT or the bHLHAB region of ARNT (Table 1). These results are consistent with our

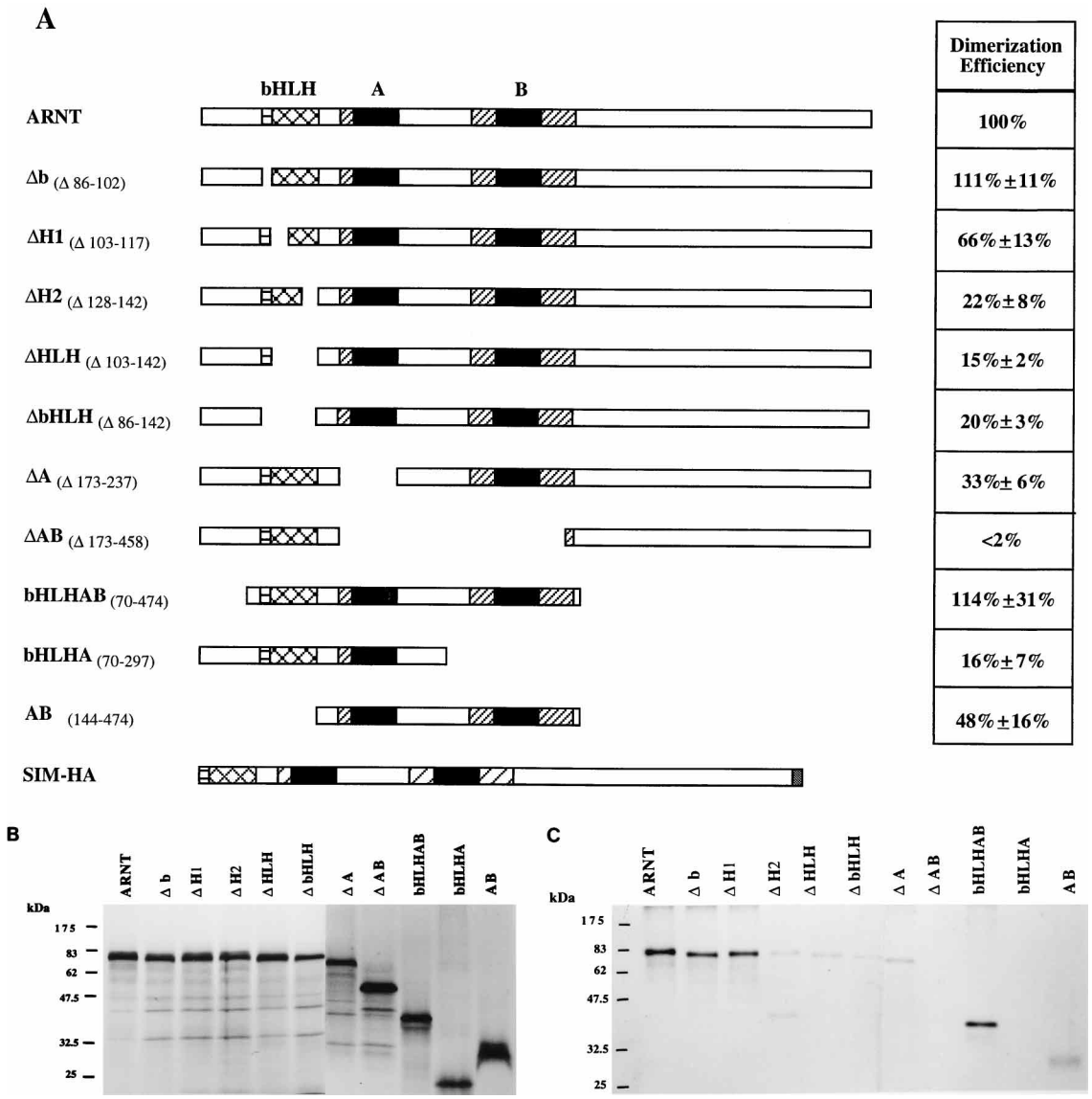

FIG. 2. Association of mARNT deletion mutants with mSIM-2. (A) Schematic representation of mARNT mutants used in this study (47). The boundary defined by deleted amino acids is indicated in parentheses as subscripts to the name of each construct. Solid boxes represent the PAS A and PAS B direct repeats, and hatched areas flanking the repeats represent extended sequence similarity to the PER, AHR and SIM proteins. Cross-hatched boxes represent the HLH domain, and horizontally lined boxes represent the basic region. The HA epitope tag is represented by a gray box. The association efficiency was calculated by comparing the percentage of coimmunoprecipitated ARNT deletion mutant relative to wild-type ARNT, which was set as 100%. The results represent the mean of at least three independent experiments. (B) Analysis of ARNT translation products. Equimolar amounts of translation products were analyzed by SDS-PAGE (12% polyacrylamide) followed by fluorography and autoradiography. The relative molecular masses of protein standards are indicated to the left. (C) Analysis of mARNT coimmunoprecipitated products by using unlabeled SIM-HA and the anti-HA antibody, 12CA5. Prior to the IP, unlabeled SIM-HA was incubated with the radiolabeled mARNT products indicated at the top of each lane. SIM-HA in vitro translations were monitored by performing parallel reactions in the presence of [^{35}S]methionine. Following co-IP, the proteins were analyzed by SDS-PAGE (12% polyacrylamide) and visualized by fluorography and autoradiography. Relative molecular masses of protein standards are indicated to the left (New England Biolabs prestained broad range markers).

in vitro association data (Fig. 1 and 2) and demonstrate that the bHLHAB domains of both proteins are sufficient to achieve association in vivo. The reason for the increased β-galactosidase levels observed with DNA binding vectors expressing mSIM-2 bHLHAB, relative to full-length mSIM-2, in the presence of ARNT is not well understood but may be due to the presence of a potent transcription repression domain located within the mSIM-2 carboxy terminus (see below). Consistent with in vitro co-IP results (Fig. 3), no self-association of mSIM-2 was observed in vivo (Table 1).

To corroborate the results obtained above and demonstrate in vivo association between mSIM-2 and ARNT in mammalian cells, COS-7 cells were transfected with expression vectors driving synthesis of HA-tagged ARNT and SIM bHLHAB (with no HA tag). Following radiolabeling of total cell proteins with [^{35}S]methionine, extracts were prepared and used in IP reactions with a control antibody (anti-myc; 9E10) (Fig. 4, lanes 1 to 4) or anti-HA antibody (12CA5) (lanes 5 to 8). Neither HA-ARNT nor SIM bHLHAB was immunoprecipitated by the anti-myc antibody (lanes 2 to 4). However, HA-ARNT was clearly present in extracts from HA-ARNT-transfected cells which had been immunoprecipitated with 12CA5 (lanes 6 and 7). Whereas SIM bHLHAB was not recognized by 12CA5 (lane 8), it was precipitated from extracts containing

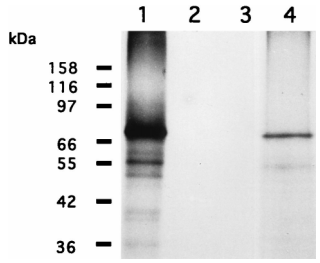

FIG. 3. MSIM-2 does not self-associate in vitro. IPs with 12CA5 were performed with radiolabeled SIM-HA (lane 1), radiolabeled mSIM-2 and unlabeled SIM-HA (lane 2), and radiolabeled mSIM-2 and unprogrammed reticulocyte lysate (lane 3). The immunoprecipitated pellets (lanes 1 to 3), as well as one-fifth of the supernatant from the [^{35}S]methionine mSIM-2/SIM-HA IP reaction loaded in lane 2 (lane 4), were analyzed by SDS-PAGE (10% polyacrylamide). Proteins were visualized by fluorography and autoradiography. Relative molecular masses of protein standards are indicated to the left.

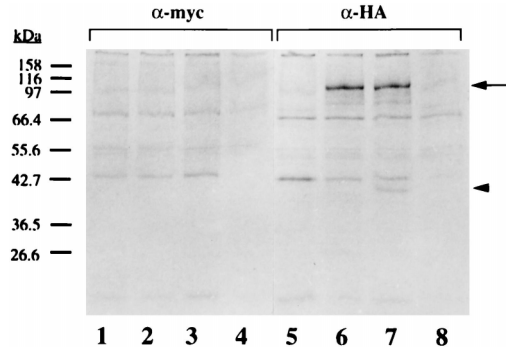

FIG. 4. In vivo association between mSIM-2 and HA-ARNT. COS-7 cells were transfected with expression vectors driving the synthesis of HA-ARNT and/or SIM bHLHAB. At 48 h after transfection, the cells were labeled with [^{35}S]methionine (100 μCi/ml) for 4 h, washed in phosphate-buffered saline, and lysed in IP buffer (see Materials and Methods). Extracts were incubated with either anti-myc (α-myc) (9E10) (lanes 1 to 4) or anti-HA (α-HA) (lanes 5 to 8) antibodies, captured with protein G-Sepharose, and processed as described in Materials and Methods for in vitro association studies. The products were analyzed by SDS-PAGE (10% polyacrylamide). The extracts were prepared from cells transfected with empty expression vector (lanes 1 and 5), pACTAG-2/mARNT (lanes 2 and 6), pACTAG-2/mARNT and SIM bHLHAB (lanes 3 and 7), and SIM bHLHAB (lanes 4 and 8). The HA-ARNT product is indicated by an arrow, and the SIM bHLHAB product is indicated by an arrowhead. Proteins were visualized by fluorography and autoradiography. Relative molecular masses of protein standards are indicated to the left (New England Biolabs broad-range markers).

HA-ARNT (lane 7). These results indicate that mSIM-2 and ARNT complexes can form in vivo.

mSIM-2 harbors two independent repression domains. To investigate the transcriptional properties of mSIM-2, we generated a series of mSIM-2 deletion mutants fused to the DBD of the yeast GAL4 transcription factor (aa 1 to 147) (Fig. 5A). These chimeric fusions allowed us to investigate the transcriptional behavior of mSIM-2 under well-defined conditions. We initially assessed the transcriptional behavior of mSIM-2 with two reporter constructs, pTECAT/5×Gal4 and TK(2×Gal4)/CAT (Fig. 5A). These reporters differ in that one contains five Gal4 binding sites immediately upstream of the TK promoter (pTECAT/5×Gal4) whereas the other contains two Gal4 DNA binding sites downstream of the TK initiation site [TK(2×Gal4)/CAT]. These two reporters were used to determine if the binding-site context influenced mSIM-2 transcriptional response. In addition, the reporter pTECAT, which lacks Gal4 binding sites, served as a negative control.

Our series of GAL4/SIM-2 expression vectors (Fig. 5A) was cotransfected with appropriate reporter constructs into COS-7 cells. A summary of relative conversion levels, obtained from at least three independent experiments, is presented in Fig. 5B. An expression vector driving the synthesis of only the Gal4 DBD (GAL4) had no effect on the levels of CAT produced from either pTECAT, pTECAT/5×Gal4, or TK(2×Gal4)/CAT (Fig. 5B). The GAL4/SIM fusion product was capable of repressing expression four- to fivefold from both pTECAT/5×Gal4 and TK(2×Gal4)/CAT but not from pTECAT, indicating that repression is dependent on the presence of Gal4 binding sites within the reporter vector (Fig. 5B).

TABLE 1. In vivo interaction between mSIM-2 and mARNT in the yeast two-hybrid system

Activation vectors	β-Galactosidase activity (Miller units)[a] for GAL4 DBD fusions:		
	pGBT9	pGBT9/SIM	pGBT9/SIM (bHLHAB)
pGAD	ND	0.023 ± 0.005	0.012 ± 0.001
pACT II	ND	0.022 ± 0.001	0.030 ± 0.005
pACT II/ARNT	0.030 ± 0.001	0.796 ± 0.036	83.97 ± 1.56
pACT II/ARNT bHLHAB)	0.015 ± 0.001	0.645 ± 0.017	30.24 ± 1.34
pGAD/SIM	0.050 ± 0.020	0.024 ± 0.001	ND
pGAD/SIM (bHLHAB)	0.032 ± 0.002	0.023 ± 0.005	0.023 ± 0.005

[a] Results are expressed in β-galactosidase units obtained as described in Materials and Methods and were done in triplicate.
[b] ND, not determined.

Deletions affecting the bHLH region (GAL4/Δb, GAL4/ΔbH1, and GAL4/ΔbHLH) or individual PAS repeats (GAL4/ΔB and GAL4/BC), or a missense mutation in PAS A (GAL4/SIML), did not affect the repression potential of mSIM-2 (Fig. 5B). Deletions of the carboxyl terminus of mSIM-2 (GAL4/bHLHAB and GAL4/bHLHA) produced fusion proteins that were no longer capable of repressing either TK(2×Gal4)/CAT or pTECAT/5×Gal4, consistent with the presence of a repressor element(s) within this region. Two constructs in which the entire PAS domain was deleted, GAL4/ΔAB and GAL4/SIMC, produced fusion proteins consistently demonstrating a slightly stronger *trans*-repression activity on pTECAT/5×Gal4 and TK(2×Gal4)/CAT than GAL4/SIM (two- to threefold greater). This increased activity, relative to that observed for GAL4/SIM, was also observed for TK(2×Gal4)/CAT in HeLa, NIH 3T3, and 293 cells (41a), indicating that it is not a cell-specific phenomenon (pTECAT/5×Gal4 was tested only in COS-7 cells). We interpret our results to indicate that mSIM-2 contains a potent *trans*-repression element(s) within the carboxyl terminus (aa 359 to 657).

To define the domain(s) within the mSIM-2 carboxyl terminus responsible for *trans*-repression, we generated an additional series of deletion mutants. The carboxy terminus of mSIM-2 can be arbitrarily divided into three regions, each enriched for specific amino acids; serine-threonine (ST) (aa 348 to 369), proline-serine (PS) (aa 384 to 503), and proline-alanine (PA) (aa 504 to 644). A series of expression vectors in which these domains were fused to the GAL4 DBD were generated and cotransfected with pTECAT/5×Gal4 or TK(2×Gal4)/CAT into COS-7 cells (Fig. 6A to C). Whereas GAL4/SIMC inhibited CAT expression from pTECAT/5×Gal4 and TK(2×Gal4)/CAT approximately 10-fold, no effect was observed on pTECAT, attesting to the absolute requirement for DNA binding to achieve inhibition. Deletion of the ST-rich region had little effect on the *trans*-repression ac-

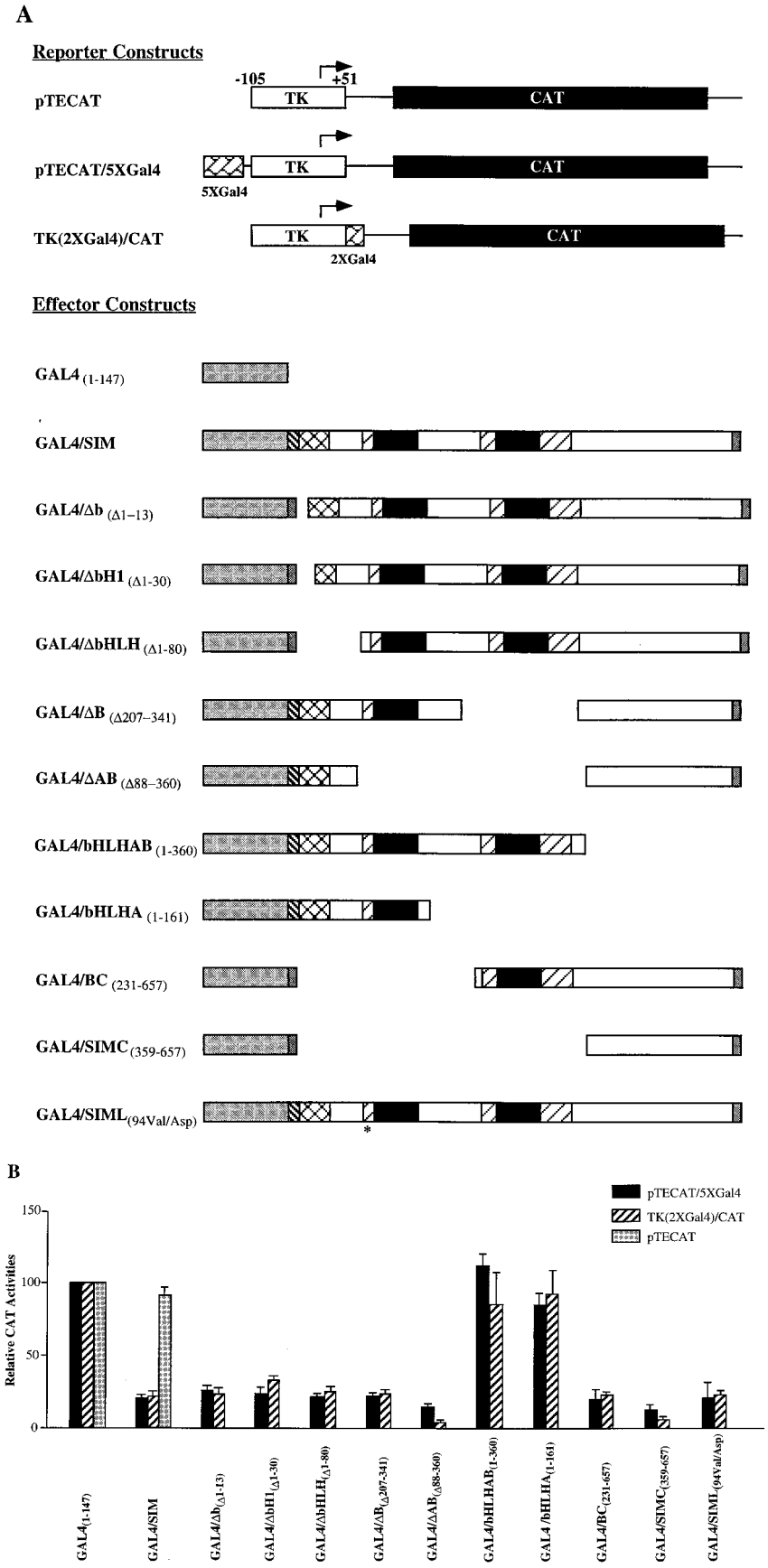
A
Reporter Constructs
-105
+51
pTECAT
TK
CAT
pTECAT/5XGal4
5XGal4
TK(2XGal4)/CAT
2XGal4
Effector Constructs
GAL4 (1-147)
GAL4/SIM
GAL4/Δb (Δ1–13)
GAL4/ΔbH1 (Δ1-30)
GAL4/ΔbHLH (Δ1-80)
GAL4/ΔB (Δ207–341)
GAL4/ΔAB (Δ88–360)
GAL4/bHLHAB (1-360)
GAL4/bHLHA (1-161)
GAL4/BC (231-657)
GAL4/SIMC (359-657)
GAL4/SIML (94Val/Asp)
B
pTECAT/5XGal4
TK(2XGal4)/CAT
pTECAT
Relative CAT Activities
150
100
50
0
GAL4(1-147)
GAL4/SIM
GAL4/Δb(Δ1-13)
GAL4/ΔbH1(Δ1-30)
GAL4/ΔbHLH(Δ1-80)
GAL4/ΔB(Δ207-341)
GAL4/ΔAB(Δ88-360)
GAL4/bHLHAB(1-360)
GAL4/bHLHA(1-161)
GAL4/BC(231-657)
GAL4/SIMC(359-657)
GAL4/SIML(94Val/Asp)

tivity (compare GAL4/SIM-PS-PA to GAL4/SIMC). Consistent with this data, expression of GAL4/SIM-ST was unable to repress either pTECAT/5×Gal4 or TK(2×Gal4)/CAT. However, expression of both the ST- and PS-rich regions (GAL4/SIM-ST-PS) repressed CAT expression as efficiently as GAL4/SIMC, indicating the presence of a repression domain. In addition, expression of the PA region fused to GAL4 efficiently repressed expression from pTECAT/5×Gal4 and TK(2×Gal4)/CAT, indicating the presence of a second independent repression domain. A deletion at the carboxy terminus of the PA domain, removing 49 aa, produced a polypeptide (GAL4/SIM-PAΔS) that was no longer capable of effectively repressing transcription. Western blot analysis revealed that GAL4/SIM-ST (lane 3), GAL4/SIM-ST-PS (lane 4), GAL4/SIM-PA (lane 5), and GAL4/SIM-PAΔS (lane 6) produced approximately similar levels of protein, but more than GAL4/SIMC (lane 1) and GAL4/SIM-PS-PA (lane 2). The repression behavior of the various constructs does not correlate with protein levels (Fig. 6D). These results have been reproduced for the reporter TK(2×Gal4)/CAT in a number of cell lines, including HeLa (human cervical carcinoma), NIH 3T3 (mouse fibroblast) and human 293 (fetal kidney) cells (41a), demonstrating that this effect is not cell type specific (pTECAT/5×Gal4 was tested only in COS-7). We interpret these results to indicate that mSIM-2 contains at least two separable repression domains within the carboxyl terminus; one in the PA-rich region, and one in the ST/-PS-rich region.

Dominant repression by mSIM-2 through association with ARNT. Preliminary experiments have suggested that mSIM-2 can repress activation by ARNT when cotransfected into COS-7 cells (16), although the mechanism or specificity of the effect was not defined. We investigated the effect of mSIM-2 on ARNT-mediated transactivation by using a mammalian two hybrid system (Fig. 7A). In this setting, DNA binding and transactivation is mediated by a GAL4/ARNT fusion (*Bait Construct*). GAL4/ARNT is capable of activating transcription when cotransfected with the minimal promoter reporter construct, 5×Gal4/E1B/CAT (Fig. 7B, compare lane 2 to lane 1), a phenomenon that has been well characterized (30, 59). When full-length mSIM-2 is introduced in this assay, ARNT-mediated activation is efficiently abrogated (compare lane 3 to lane 2). This effect is dependent on the presence of the mSIM-2 carboxy terminus, since it is not observed with the truncation mutant SIM bHLHAB (compare lane 4 to lanes 2 and 3). Repression is also dependent on the ability of ARNT and mSIM-2 to associate, since mSIM-2 mutants incapable of interacting with ARNT (SIM ΔbHLH and SIM ΔB) fail to repress ARNT-mediated transactivation (compare lanes 5 and 6 to lane 2). Similar results with these constructs were obtained with HeLa and NIH 3T3 cells, indicating that this effect is not cell type specific (41a). These results indicate that mSIM-2 can actively repress ARNT-mediated transactivation, possibly by quenching ARNT activity and/or acting directly upon the basal transcription apparatus.

To address whether the observed inhibition was specific for the ARNT activation domain, we replaced the glutamine-rich activation domain of ARNT with the acidic activation domain of GAL4 (GAL4/ARNT/GAL4) (Fig. 7A). Like GAL4/ARNT, cotransfection of GAL4/ARNT/GAL4 stimulated 5×Gal4/E1B/CAT reporter activity (Fig. 7C, compare lane 2 to lane 1). Introduction of mSIM-2 (or deletion mutants) into this system revealed that mSIM-2, but not SIM ΔbHLH or SIM ΔAB, was capable of abrogating activation by GAL4/ARNT/GAL4 (compare lanes 4 and 5 to lane 3). These results suggest that the repression activity of mSIM-2 is not specific to the activation domain of its putative binding partner, ARNT.

To assess if DNA recruitment of mSIM-2 is sufficient to directly inhibit expression from a promoter with high basal activity, in contrast to quenching of ARNT *trans*-activation function, a truncation mutant of GAL4/ARNT lacking the carboxy-terminal activation domain, GAL4/ARNT(bHLHAB), was used in the mammalian two-hybrid system. In this assay, we used the TK promoter since it has a high basal activity (Fig. 7D, lane 1). In the presence of TK(2×Gal4)/CAT, GAL4/ARNT-(bHLHAB) had a minimal effect (~twofold reduction) on CAT expression (compare lane 2 to lane 1). This slight inhibition is probably nonspecific since it was also observed with the reporter pTECAT/5×Gal4 (1.5-fold) (41a). Introduction of a vector driving the expression of mSIM-2 resulted in significant repression of TK activity (~5- to 10-fold; compare lane 3 to lane 2). This repression was dependent on the presence of the mSIM-2 carboxy terminus (compare lane 4 to lane 3), as well as on the ability of mSIM-2 to associate with ARNT, since mutants ΔbHLH and ΔAB failed to inhibit CAT expression (compare lanes 5 and 6 to lane 3). These results are consistent with a mechanism whereby mSIM-2/ARNT heterodimers bind to DNA, and the potent mSIM-2 repression domains inhibit transactivation by ARNT and/or of adjacent *trans*-acting factors.

Interference of HIF-1α activity by competition for ARNT by mSIM-2. Recent experiments by Gradin et al. (21) have demonstrated that HIF-1α can functionally interfere with the dioxin signaling pathway by competing with AHR for recruitment of ARNT. To assess whether mSIM-2 could similarly compete with HIF-1α for ARNT, we established the following assay. Hif-1α, GAL4/ARNT bHLHAB, and 5×Gal4/E1B/CAT were cotransfected with various mSIM-2 derivatives into COS-7 cells. In the presence of $CoCl_2$, which mimics hypoxic conditions where Hif-1α is activated, GAL4/ARNT bHLHAB alone or in combination with mSIM-2 had little effect on gene expression from 5×Gal4/E1B/CAT (Fig. 8, compare lanes 2 and 3 to lane 1). In contrast, coexpression of GAL4/ARNT bHLHAB and Hif-1α significantly stimulated CAT expression (~20-fold; compare lane 4 to lane 2). This effect was not observed under normoxic conditions (41a). Addition of mSIM-2 to the transfection mixture significantly inhibited the Hif-1α/ARNT-mediated transcriptional response (compare lane 5 to lane 4). This effect was also observed with the deletion mutant SIM bHLHAB but not with SIM ΔB (compare lanes 6 and 7 to lanes 4 and 5). Since bHLHAB, but not ΔB, is capable of associating with GAL4/ARNT bHLHAB, we inter-

FIG. 5. Transcriptional repression by mSIM-2. (A) Schematic representation of reporter and effector vectors. The TK promoter is represented by open boxes, Gal4 binding sites are represented by boxes with patches, and the CAT gene is represented by a solid box. A right-angled arrow indicates the transcriptional start site. Nucleotide positions demarcate the boundaries of the TK promoter, which are identical in all three reporter constructs. The Gal4 DBD is represented by light gray boxes, and HA epitopes are represented by darker gray boxes. Solid boxes in the mSim-2 coding region denote the PAS repeats, and lightly hatched boxes represent extended sequence similarity to the PER, AHR, and ARNT proteins. Cross-hatched boxes represent the HLH region, and darkly hatched boxes represent the DNA binding basic region. (B) *trans*-repression of the pTECAT, pTECAT/5×Gal4, and TK/(2×Gal4)/CAT reporter constructs by GAL4/mSIM-2 fusion proteins. COS-7 cells were transfected with 3 μg of reporter vector and 5 μg of effector plasmid for these studies. The expression plasmids used in the *trans*-repression studies are indicated below the panel, and the key for the reporter vectors is illustrated at the top right. CAT activity was normalized to the activity obtained with GAL4, which was set at 100%. The results are the means of at least three separate experiments.

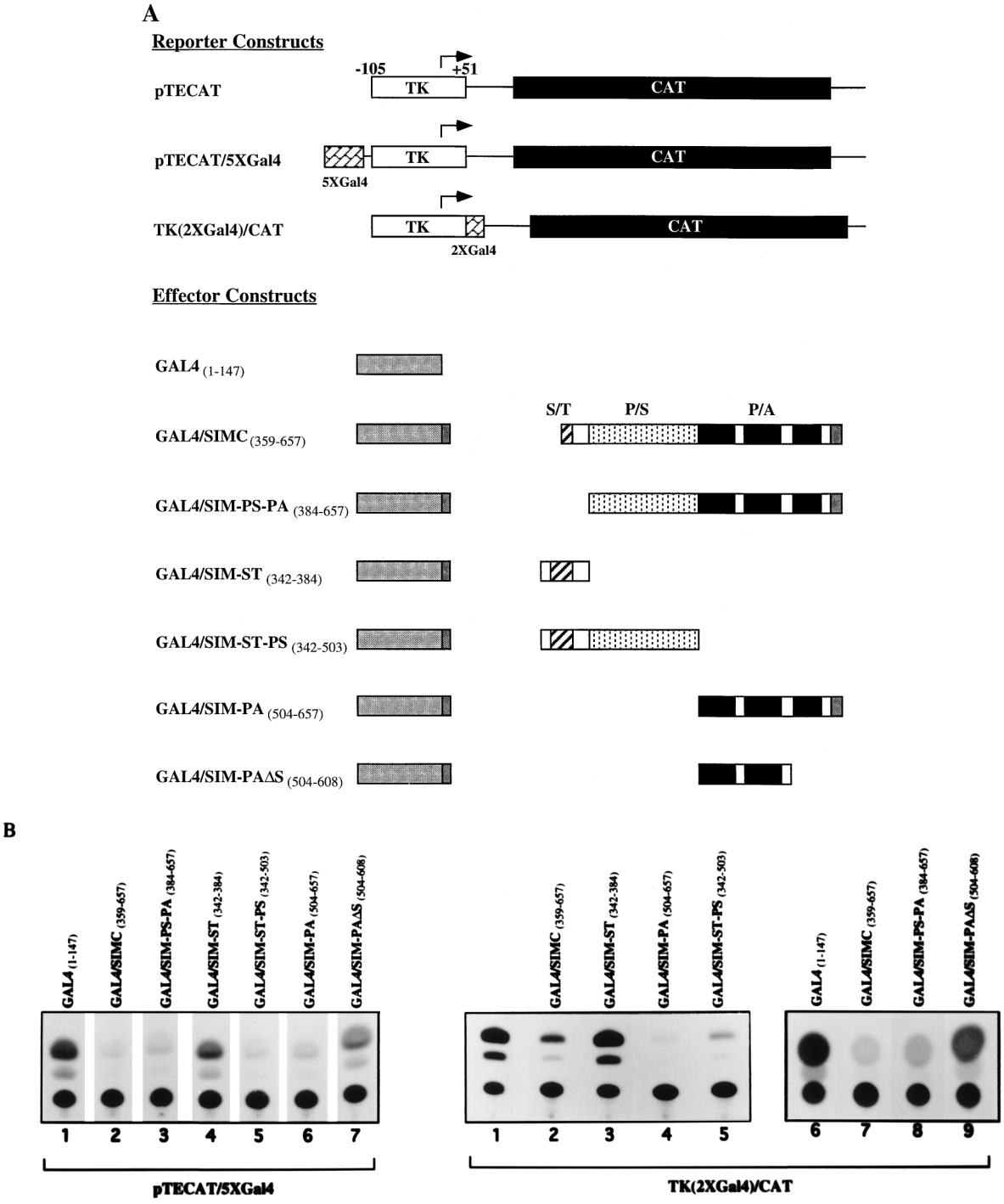

pret these results to indicate that mSIM-2 can interfere with Hif-1α/ARNT transactivation by complexing to ARNT. This repression mechanism is clearly distinct from that defined above (Fig. 5 to 7).

DISCUSSION

Association of mSIM-2 and mARNT. Previous studies have documented the ability of DSIM to associate with mARNT (15, 40, 51, 52). We have confirmed that mARNT can associate with mSIM-2 and, using fine-structure deletion mapping, have demonstrated that the HLH and PAS regions of mSIM-2 and ARNT are required for optimal association. Our results suggest that these two domains cooperate in dimerization and that extensive protein-protein contacts exist between both proteins.

The association of ARNT with AHR and HIF-1α has been critically studied with deletion mutants (19, 31, 47). We find that the domains required for mSIM-2/ARNT interaction are

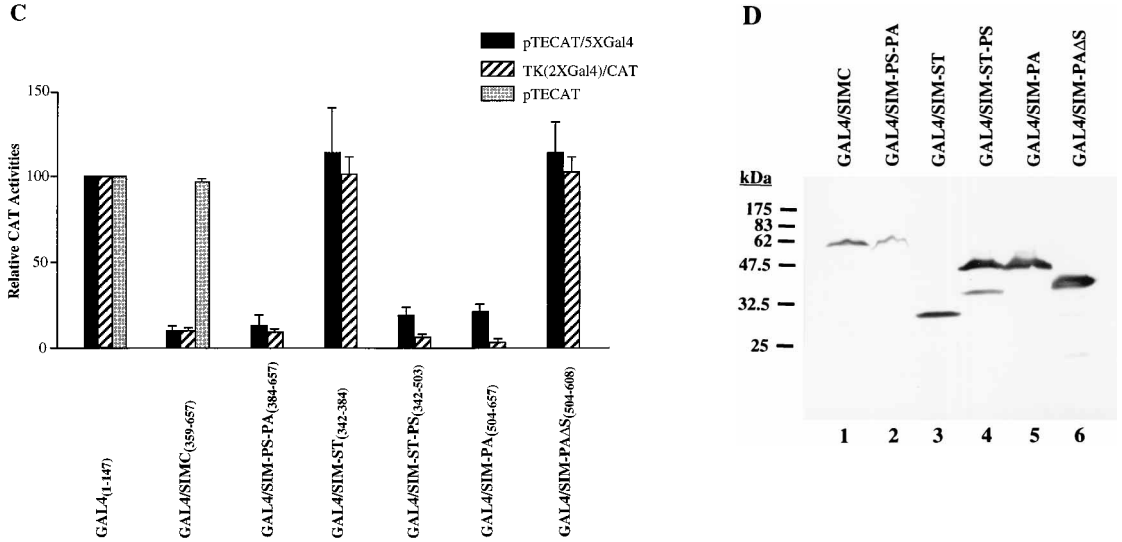

FIG. 6. Delineation of the mSIM-2 *trans*-repression domain. (A) Schematic diagram of expression vectors driving the synthesis of fusion constructs containing the GAL4 DBD fused to portions of the mSIM-2 carboxy terminus. The GAL4 DBD is represented by light gray boxes, and HA epitope tags are represented by dark gray boxes. Hatched boxes represent the ST-rich region (aa 348 to 369), stippled boxes represent the PS-rich region (aa 384 to 503), and solid boxes represent areas enriched for PA (aa 504 to 545, 554 to 596, and 611 to 644). (B) Autoradiograph of a representative thin-layer chromatogram for CAT assays in which COS-7 cells were transfected with 3 μg of pTECAT/5×Gal4 or TK(2×Gal4)/CAT and 5 μg of either GAL4 or GAL4/SIM fusions. Thin-layer chromatography of CAT assay mixtures for pTECAT/5×Gal4 were performed at the same time and on the same plate, but the order of the lanes of the photograph has been changed to present the data as shown. (C) Summary of *trans*-repression GAL4/mSIM-2 fusion proteins. Effector plasmids used in the *trans*-repression studies are indicated below the panel, and the key for the reporter vectors is illustrated at the top right. CAT activity was normalized to the activity obtained with GAL4, which was set at 100%. Results are shown for at least three separate experiments. (D) Western blot analysis of GAL4/SIM fusion proteins. Five micrograms of expression vector was transfected into COS-7 cells as described previously (49). At 48 h after transfection, the cells were harvested in SDS sample buffer (33), DNA was sheared by passing the extract through a 25-gauge needle 10 times, and samples were analyzed on SDS–10% polyacrylamide gel. Following transfer of proteins to Immobilon P membrane, the blot was preblocked overnight at 4°C in TBST (10 mM Tris-HCl [pH 8.0], 150 mM NaCl, 0.5% Tween 20) containing 5% skim milk and probed with anti-Gal4 antibodies (Santa Cruz) (1:1,000). Following extensive washing with TBST, the blot was developed with an enhanced chemiluminescence (ECL) kit from Amersham and horseradish peroxidase-conjugated anti-mouse antibodies (1:7,500) (Santa Cruz). The expression vectors used to transfect COS-7 cells are indicated above each panel. Relative molecular masses of protein standards are indicated to the left.

similar but not identical to those required for AHR/ARNT association (19, 47). (i) One difference relates to the requirement of the HLH domains of mSIM-2 and AHR for ARNT association. Whereas deletions of either helix or of the complete AHR HLH domain abolishes ARNT association, similar deletions in the mSIM-2 HLH region reduced but did not entirely abrogate ARNT interaction (Fig. 1). (ii) Deletion of the first ARNT helix (ΔH1) results in complete abrogation of AHR dimerization (47), whereas the same mutant is still capable of efficiently associating with mSIM-2 (Fig. 2). While deletion of the first helix of most HLH proteins results in complete abrogation of the dimerization potential, this is not a universal phenomenon. For example, deletion of the first helix in the HLH domain of MyoD results in a mutant which is still capable of binding to Id, albeit with reduced efficiency (4). (iii) The PAS A repeat has been postulated to serve as a spacer region in AHR and ARNT (19, 47), since AHR deletion mutants lacking this region can interact with similar ARNT mutants. However, we find that PAS A probably plays an important role in mSIM-2/ARNT interactions since a missense mutation within the PAS A repeat severely disrupted the mSIM-2/ARNT association (Fig. 1, SIML). This mutation, modeled after the *Per*^{L} mutation, which lengthens the circadian rhythm of *Drosophila*, disrupts the dimerization properties of the PER protein (28). Since in this scenario the mSIM-2 PAS A repeat should still be capable of functioning as a spacer, the reduction in the association between SIML and ARNT suggests an active role for the mSIM-2 PAS A repeat in the mSIM-2/ARNT interaction. Of course, we cannot exclude the formal possibility that the SIML mutation has a significant effect on SIM protein conformation. (iv) There is also a noticeable difference between ARNT/HIF-1α and ARNT/SIM-2 association requirements. Whereas the bHLH and PAS A domains of HIF-1α are sufficient for dimerization with ARNT (31), such is not the case for mSIM-2 (or AHR [19]), where PAS B is also required (Fig. 1). We interpret these differences to indicate that the AHR and HIF-1α interaction sites on ARNT overlap, but are distinct, from the mSIM-2 binding site.

Although AHR/ARNT interactions require the presence of an AHR ligand (for a review, see reference 23), no such ligand has yet been identified for mSIM-2. It is thus unclear if mSIM-2 is an orphan receptor or if the mSIM-2/ARNT interaction is dependent on the presence of an endogenous ligand. If the latter were the case, such a ligand would be predicted to be relatively common, since mSIM-2 and ARNT can interact in a number of systems, including several mammalian cell lines, yeast, and rabbit reticulocyte lysate.

DSIM and mSIM-1 associate with HSP90 (40, 45); however, no studies have yet been reported for mSIM-2. It is likely that mSIM-2 also interacts with HSP90, although not all closely related PAS-containing proteins share similar HSP90 binding properties (27). If mSIM-2 interacts with HSP90, our association studies with mSIM-2 deletion mutants do not allow us to formally distinguish between putative effects of HSP90 on dimerization efficiencies with mSIM-2 versus direct effects on ARNT/mSIM-2 association and so should be interpreted with caution. In any event, our data is internally consistent in that the bHLHAB of both proteins is required for optimal association in vitro (Fig. 1 and 2) as well as in vivo (Fig. 3 and 4). The consequence of deletions which affect the integrity of the bHL-

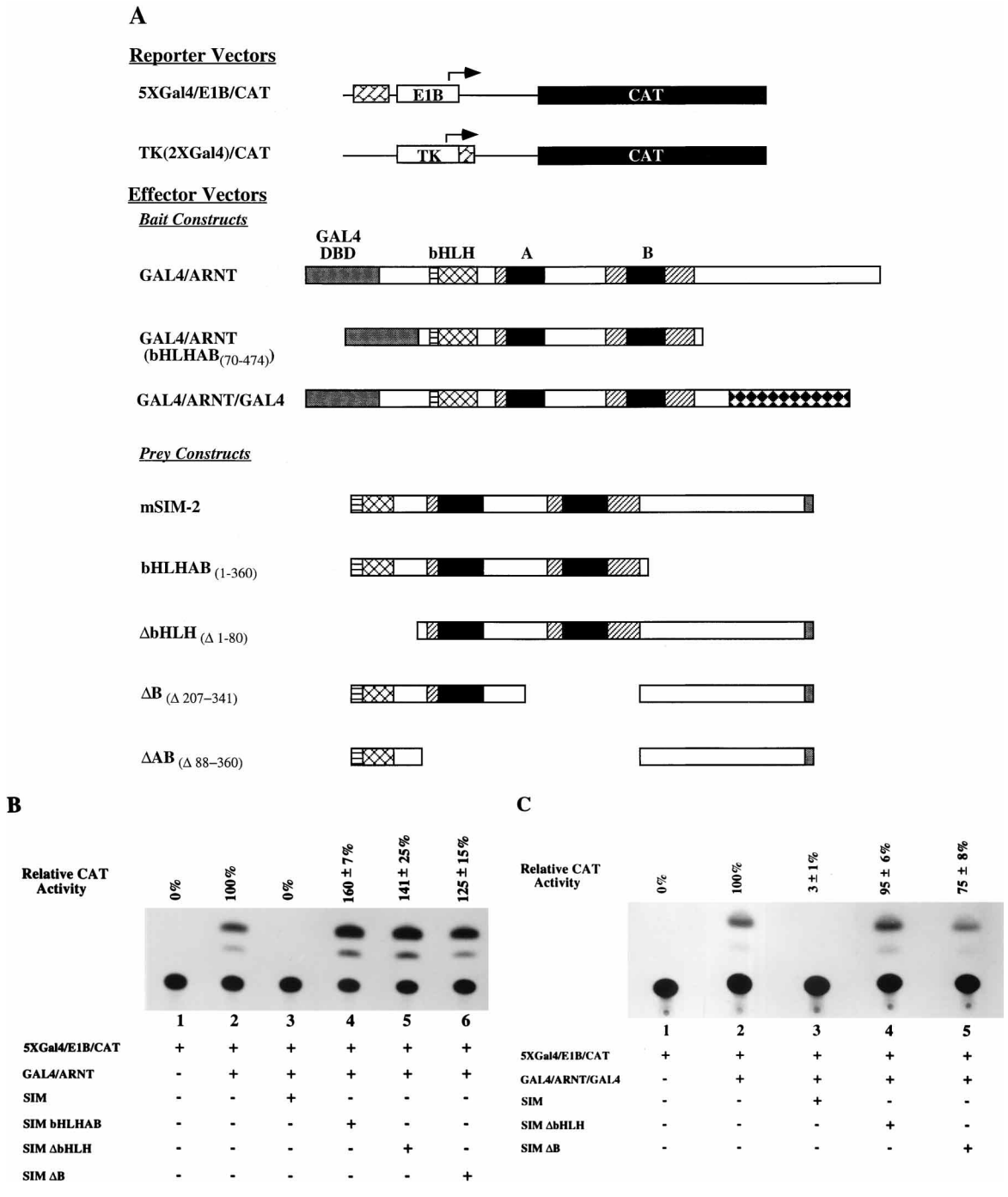

HAB region is more difficult to predict, given our limited understanding of the structure and function of this domain.

***trans*-repression by mSIM-2.** We have shown that the carboxy terminus of mSIM-2, when fused to a heterologous DBD, contains at least two independent domains capable of repressing gene expression from the activated TK promoter (Fig. 5 and 6). These two domains, encompassed by aa 384 to 503 and aa 504 to 657, have a high proline/serine and proline/alanine content, respectively. Such features are characteristic of "repressor motifs" and are found in a large number of other transcriptional repressors (for a review, see reference 24). We also find that removal of the last 49 aa from the proline-alanine region abolished the activity of this repression domain (Fig. 6, compare GAL4/SIM-PAΔS to GAL4/SIMPA).

We find that the repression activity of mSIM-2 is slightly increased (two- to threefold) when the PAS domains are removed (Fig. 6B, compare GAL4/SIMC or GAL4/ΔAB to GAL4/SIM). A modulatory role by a PAS domain would not be exclusive to mSIM-2, since inhibition of transactivation has been previously shown for the PAS domains of DSIM (18) and AHR (30, 38, 57). The mechanism by which mSIM-2 repression may be modulated by PAS domains remains to be investigated.

Since physiologically relevant targets of mSIM-2 are not

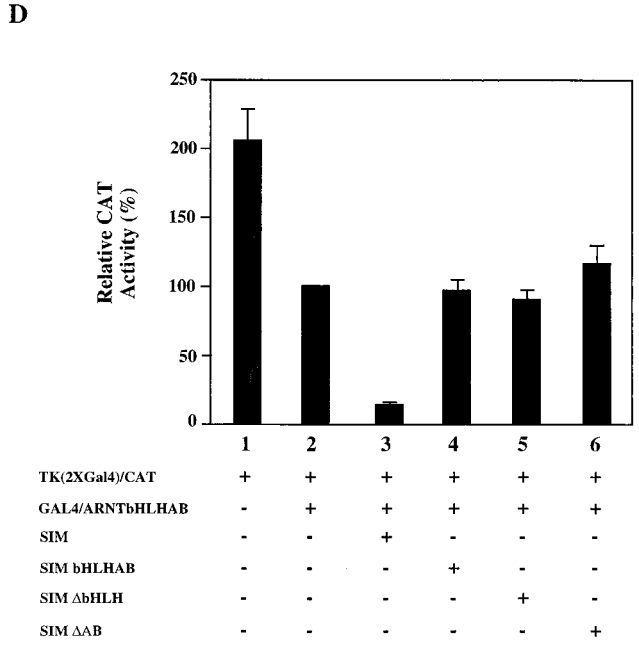

FIG. 7. Inhibition of ARNT-mediated transactivation by mSIM-2. (A) Schematic diagram of the constructs used. For reporter constructs, solid boxes represent the CAT gene, open boxes represent the E1B minimal and TK promoters, and boxes with patches represent Gal4 binding sites. For expression vectors, darkened boxes represent the PAS A and PAS B direct repeats and hatched areas flanking the repeats represent extended sequence similarity to the PER, AHR, and ARNT proteins. Cross-hatched boxes represent the HLH domain, and horizontally lined boxes represent the basic domain. The GAL4 DBD is illustrated by gray shaded boxes, and the GAL4 transactivation domain is represented by cross-hatched checkered boxes. (B) A representative thin-layer chromatogram illustrating mSIM-2 inhibition of ARNT-mediated activation. COS-7 cells were transfected with 3 μg of 5×Gal4/E1B/CAT and 12 μg of pcDNA3 (lane 1), 3 μg of GAL4/ARNT plus 9 μg of pcDNA3 (lane 2), and 3 μg of GAL4/ARNT plus 9 μg of the indicated mSim-2 expression vectors (lanes 3 to 6). The percent CAT conversion indicated above the TLC plate is the value obtained from three independent experiments, with the values normalized to the transfection containing GAL4/ARNT and pcDNA3 (lane 2), which has been set at 100%. (C) A representative thin-layer chromatogram illustrating mSIM-2 inhibition of GAL4/ARNT/GAL4 activation. COS-7 cells were transfected with 3 μg of 5×Gal4/E1B/CAT and 12 μg of pcDNA3 (lane 1), 3 μg of GAL4/ARNT/GAL4 plus 9 μg pcDNA3 (lane 2), and 3 μg of GAL4/ARNT/GAL4 plus 9 μg of the indicated mSIM-2 constructs (lanes 3 to 5). The percent CAT activity indicated above the plate is the mean value obtained from three independent experiments, with the values normalized to the transfection containing GAL4/ARNT/GAL4 + pcDNA3 (lane 2), which has been set at 100%. (D) Inhibition of TK promoter activity mediated by mSIM-2/ARNT association. COS-7 cells were transfected with 3 μg of TK(2×Gal4)/CAT and 12 μg of pcDNA3 (lane 1), 3 μg of GAL4 ARNT(bHLHAB) plus 9 μg of pcDNA3 (lane 2), and 3 μg of GAL4 ARNT(bHLHAB) plus 9 μg of the indicated mSim-2 expression vectors (lanes 3 to 6). The percent CAT conversion indicated is the value obtained from three independent experiments, with values normalized to the transfection containing TK(2×Gal4)/CAT plus GAL4 ARNT(bHLHAB) plus pcDNA3 (lane 2), which has been set at 100%.

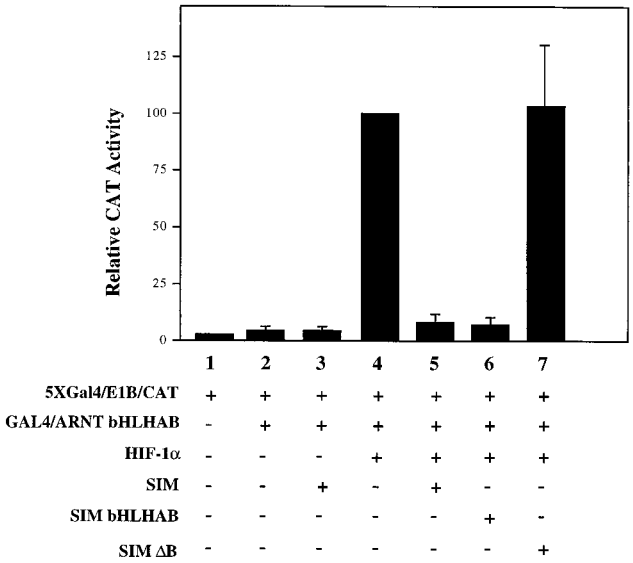

FIG. 8. Interference of HIF-1α activity by mSIM-2. COS-7 cells were transfected with 3 μg of 5×Gal4/E1B/CAT (lanes 1 to 7), 2 μg of GAL4/ARNT bHLHAB (lanes 2 to 7), 3 μg of HIF-1α expression vector (lanes 4 to 7), and 6 μg of the indicated mSim-2 expression vectors (lanes 3 and 5 to 7) and grown in the presence of 200 μM $CoCl_2$ for 24 h before being harvested. The total amount of DNA in each transfection was equalized by compensating with the empty expression vector, pcDNA3. The amount of CAT conversion of each lane is set relative to that obtained with 5×Gal4/E1B/CAT plus GAL4/ARNT bHLHAB plus HIF-1α (lane 4), which was set at 100%. Values were obtained from three independent experiments and have been standardized to β-galactosidase values.

known, it is difficult to predict the architecture of putative promoters under mSIM-2 regulation. We have therefore assessed the transcriptional properties with reporters in which DNA recognition sites were upstream (pTECAT/5×Gal4) or downstream (TK(2×Gal4)/CAT) of the transcription initiation sites (Fig. 5 and 6). We believed that it was important to assess the effects of mSIM-2 on a reporter with DNA binding sites downstream of transcription initiation, since recognition motifs in this context have been described for well-known transcription factors (e.g., regulation of the PDGF-A promoter by the WT1 tumor suppressor gene product [reviewed in reference 46], c-myc regulation by hCUT [39], and ICP4-mediated repression [22]). Although we cannot formally conclude that the mechanism of repression by mSIM-2 is identical for both reporters, all deletion mutants of mSIM-2 behaved similarly with both constructs. It is unlikely that occlusion of RNA polymerase is occurring in TK(2×Gal4)/CAT, since not all GAL4/SIM deletions inhibit transcription (Fig. 5 and 6). Defining the mechanism of action of mSIM-2 on pTECAT/5×Gal4 and TK(2XGal4)/CAT will require more detailed analysis. Nevertheless, our results illustrate the presence of two potent repression domains within the mSIM-2 carboxy terminus which function whether positioned upstream or downstream of transcription initiation sites.

Transcriptional repression can occur by several general mechanisms. These include (i) occlusion of DNA binding by competition with a transactivator for a common DNA binding site; (ii) interference (or squelching) by sequestration of an activator or an essential cofactor (the squelching phenomenon is not DNA binding dependent); (iii) quenching, in which a repressor bound to a given target suppresses transactivation by interacting with an adjacent transactivator, thereby preventing the transactivator from interacting with the basal transcription machinery; and (iv) direct repression by interference with the formation or activity of the basal transcription complex, either directly or through recruitment of a corepressor.

Our results indicate that mSIM-2 probably represses transcription by two mechanisms: active repression and interference (Fig. 5 to 8). Although these mechanisms were elucidated with "model" reporter constructs, our studies are useful in terms of defining the structural and functional requirements for mSIM-2 behavior. Using a mammalian two-hybrid system, we demonstrate that ARNT-mediated transactivation is severely impaired in the presence of mSIM-2. This effect is dependent on the presence of the mSIM-2 carboxy-terminal domain. Our data is not consistent with a specific quenching

mechanism, since repression by mSIM-2 is not ARNT specific, being observed with the GAL4 activation domain, as well as on the activated TK promoter (Fig. 6). We therefore favor a model whereby mSIM-2 mediates its effects on the basal transcription apparatus (direct repression). The repression properties of mSIM-2 may account for the low β-galactosidase levels obtained in the yeast two-hybrid system, when full-length mSIM-2 is cointroduced with ARNT activation vectors (Table 1). A dominant effect on the activation domain of ARNT has also been previously characterized with respect to the AHR (32) and HIF-1α (31). However, in these situations, both AHR and HIF-1α are transactivators.

The majority of bHLH-PAS transcription factors so far characterized act as transcriptional activators (ARNT, ARNT2, AHR, HIF-1α, DSIM, and EPAS1/MOP2), with the responsible domain(s) residing within the carboxy-terminal moiety of the protein. We have assessed whether the mSIM-2 protein could not also harbor a transactivation domain(s) in addition to the repression domains identified in this report and have found no evidence in favor of such a domain (41a). We find that mSIM-2 can inhibit an activation signal mediated by ARNT/HIF-1α complexes through direct competition for ARNT binding (Fig. 8), referred to as interference. Interference could conceivably down-regulate hypoxia-induced (mediated by HIF-1α/ARNT complexes) or dioxin-induced (mediated by AHR/ARNT complexes) signal transduction pathways. Consistent with this model, mSIM-2 and Hif-1α are both expressed at their highest constitutive levels in the kidney (27, 41, 45), where AHR and ARNT are also present (1, 2, 6).

The human homolog of *mSim-2* maps within the Down syndrome critical region on chromosome 21 (8, 10, 37, 41). The expression profile of this gene suggests that it may play a role in some of the pathophysiology of Down syndrome. Insight into the regulation of mSIM-2 activity is thus essential to understanding if altering the stoichiometry of bHLH-PAS proteins and disturbing the normal cross-regulation of these transcription factors contributes to Down syndrome.

ACKNOWLEDGMENTS

P.M. is supported by a studentship from the Cancer Research Society. M.R. is supported by a studentship from the Fonds pour la Formation de Chercheur et L'Aide à la Recherche (FCAR). J.P. is an MRC Scholar. This work was supported by grants from the Medical Research Council and Kidney Foundation of Canada to J.P.

We thank Gregg Semenza (John Hopkins University) for his kind gift of pSK/Hif-1α and Oliver Hankinson for his kind gift of ARNT expression constructs. We thank the anonymous reviewers for their helpful suggestions in assisting with the revision of the manuscript.

REFERENCES

1. **Abbot, B. D., and M. R. Probst.** 1995. Developmental expression of two members of a new class of transcription factors. II. Expression of aryl hydrocarbon receptor nuclear translocator in the C57BL/6N mouse embryo. Dev. Dyn. **204:**144–155.
2. **Abbott, B. D., L. S. Birnbaum, and G. H. Perdew.** 1995. Developmental expression of two members of a new class of transcription factors. I. Expression of aryl hydrocarbon receptor in the C57BL/6N mouse embryo. Dev. Dyn. **204:**133–143.
3. **Antonsson, C., V. Arulampalam, M. L. Whitelaw, S. Pettersson, and L. Poellinger.** 1995. Constitutive function of the basic helix-loop-helix/PAS factor Arnt. J. Biol. Chem. **270:**13968–13972.
4. **Benezra, R., R. L. Davis, D. Lockshon, D. L. Turner, and H. Weintraub.** 1990. The protein Id: a negative regulator of helix-loop-helix DNA binding proteins. Cell **61:**49–59.
5. **Burbach, K. M., A. Poland, and C. A. Bradfield.** 1992. Cloning of the Ah-receptor cDNA reveals a distinctive ligand-activated transcription factor. Proc. Natl. Acad. Sci. USA **89:**8185–8189.
6. **Carver, L. A., J. B. Hogenesch, and C. A. Bradfield.** 1994. Tissue specific expression of the rat Ah-receptor and ARNT mRNAs. Nucleic Acid Res. **22:**3038–3044.
7. **Charest, A., J. Wagner, S. Shen, and M. Tremblay.** 1995. Murine protein tyrosine phosphatase-PEST, a stable cytosolic protein tyrosine phosphatase. Biochem. J. **308:**425–432.
8. **Chen, H., R. Chrast, C. Rossier, A. Gos, S. E. Antonarakis, J. Kudoh, A. Yamaki, N. Shindoh, H. Maeda, S. Minoshima, and N. Shimizu.** 1995. Single-minded and Down syndrome? Nat. Genet. **10:**9–10.
9. **Crews, S. T., J. B. Thomas, and C. S. Goodman.** 1988. The *Drosophila single-minded* gene encodes a nuclear protein with sequence similarity to the *per* gene product. Cell **52:**143–151.
10. **Dahmane, N., G. Charon, C. Lopes, M.-L. Yaspo, C. Maunoury, L. Decorte, P.-M. Sinet, B. Bloch, and J.-M. Delabar.** 1995. Down syndrome-critical region contains a gene homologous to Drosophila sim expressed during rat and human central nervous system development. Proc. Natl. Acad. Sci. USA **92:**9191–9125.
11. **Dolwick, K. M., H. I. Swanson, and C. A. Bradfield.** 1993. In vitro analysis of Ah receptor domains involved in ligand-activated DNA recognition. Proc. Natl. Acad. Sci. USA **90:**8566–8570.
12. **Drutel, G., M. Kathmann, A. Heron, J. C. Schwartz, and J.-M. Arrang.** 1996. Cloning and selective expression in brain and kidney of ARNT2 homologous to the Ah receptor nuclear translocator (ARNT). Biochem. Biophys. Res. Commun. **225:**333–339.
13. **Durfee, T., K. Becherer, P.-L. Chen, S.-H. Yeh, Y. Yang, A. E. Kilburn, W.-H. Lee, and S. J. Elledge.** 1993. The retinoblastoma protein associates with protein phosphatase type 1 catalytic subunit. Genes Dev. **7:**555–569.
14. **Ema, M., K. Sogawa, N. Watanabe, Y. Chujoh, N. Matsushita, O. Gotoh, Y. Funae, and Y. Fujii-Kuriyama.** 1992. cDNA cloning and structure of mouse putative Ah receptor. Biochem. Biophys. Res. Commun. **184:**246–253.
15. **Ema, M., M. Suzuki, M. Morita, K. Hirose, K. Sogawa, Y. Matsuda, O. Gotoh, Y. Saijoh, H. Fujii, H. Hamada, and Y. Fujii-Kuriyama.** 1996. cDNA cloning of a murine homologue of Drosophila single-minded, its mRNA expression in mouse development, and chromosome localization. Biochem. Biophys. Res. Commun. **218:**588–594.
16. **Ema, M., M. Morita, S. Ikawa, M. Tanaka, M. Youichi, O. Gotah, Y. Saijoh, H. Fujii, H. Hamada, Y. Kikuchi, and Y. Fujii-Kuriyama.** 1996. Two new members of the murine *sim* gene family are transcriptional repressors and show different expression patterns during mouse embryogenesis. Mol. Cell. Biol. **16:**5865–5875.
17. **Fan, C. M., E. Kuwana, A. Bulfone, C. F. Fletcher, N. G. Copeland, N. A. Jenkins, S. Crews, S. Martinez, I. Puelles, J. L. R. Rubenstein, and M. Tessier-Lavigne.** 1996. Expression patterns of two murine homologs of *Drosophila single minded* suggest possible roles in embryonic patterning and in the pathogenesis of Down syndrome. Mol. Cell. Neurosci. **7:**1–16.
18. **Franks, R. G., and S. T. Crews.** 1994. Transcriptional activation domains of the single minded bHLH protein are required for CNS midline cell development. Mech. Dev. **45:**269–277.
19. **Fukanaga, B. N., M. R. Probst, S. Reisz-Porsasz, and O. Hankinson.** 1995. Identification of functional domains of the Aryl Hydrocarbon Receptor. J. Biol. Chem. **270:**29270–29278.
20. **Gorman, C.** 1985. High efficiency gene transfer into mammalian cells, p. 143–190. *In* D. M. Glover (ed.), DNA cloning, vol. 2. IRL Press, Oxford, United Kingdom.
21. **Gradin, K., J. McGuire, R. H. Wenger, I. Kvietikova, M. L. Whitelaw, R. Toftgård, L. Tora, M. Gassmann, and L. Poellinger.** 1996. Functional interference between hypoxia and dioxin signal transduction pathways: competition for recruitment of the Arnt transcription factor. Mol. Cell. Biol. **16:**5221–5231.
22. **Gu, B., Kuddus, R., and DeLuca, N. A.** 1995. Repression of activator-mediated transcription by herpes simplex virus ICP4 via a mechanism involving interactions with the basal transcription factors TATA-binding protein and TFIIB. Mol. Cell. Biol. **15:**3618–3626.
23. **Hankinson, O.** 1995. The aryl hydrocarbon receptor complex. Annu. Rev. Pharmacol. Toxicol. **35:**307–340.
24. **Hanna-Rose, W., and U. Hansen.** 1996. Active mechanisms of eukaryotic transcription repressors. Trends Genet. **12:**229–234.
25. **Hirose, K., M. Morita, M. Ema, J. Mimura, H. Hamada, H. Fujii, Y. Saijo, O. Gotah, K. Sogawa, and Y. Fujii-Kuriyama.** 1996. cDNA cloning and tissue-specific expression of a novel basic helix-loop-helix/PAS factor (Arnt2) with close sequence similarity to the aryl hydrocarbon receptor nuclear translocator (Arnt). Mol. Cell. Biol. **16:**1706–1713.
26. **Hoffman, E. C., H. Reyes, F.-F. Chu, F. Sander, L. H. Conley, B. H. Brooks, and O. Hankinson.** 1991. Cloning of a new factor required for activity of the Ah (dioxin) receptor. Science **252:**954–958.
27. **Hogenesch, J. B., W. K. Chan, V. H. Jackiw, R. C. Brown, Y. Gu, M. Pray-Grant, G. Perdew, and C. A. Bradfield.** 1997. Characterization of a subset of the basic-helix-loop-helix-PAS superfamily that interacts with components of the dioxin signalling pathway. J. Biol. Chem. **272:**8581–8593.
28. **Huang, Z. J., I. Edery, and M. Rosbash.** 1993. PAS is a dimerization domain common to Drosophila period and several transcription factors. Nature **364:**259–262.
29. **Isaac, D. D., and D. J. Andrew.** 1996. Tubulogenesis in Drosophila: a requirement for the trachealess gene product. Genes Dev. **10:**103–117.
30. **Jain, S., K. D. Dolwick, J. V. Schmidt, and C. A. Bradfield.** 1994. Potent

transactivation domains of the Ah receptor and the Ah receptor nuclear translocator map to their carboxy termini. J. Biol. Chem. **269:**31518–31524.
31. **Jiang, B., E. Rue, G. Wang, R. Roe, and G. Semenza.** 1996. Dimerization, DNA binding, and transactivation properties of hypoxia-inducible factor 1. J. Biol. Chem. **271:**17771–17778.
32. **Ko, H. P., S. T. Okino, Q. Ma, and J. P. Whitlock, Jr.** 1996. Dioxin-induced CYP1A1 transcription in vivo: the aromatic hydrocarbon receptor mediates transactivation, enhancer-promoter communication, and changes in chromatin structure. Mol. Cell. Biol. **16:**430–436.
33. **Laemmli, U. K.** 1970. Cleavage of structural proteins during the assembly of the head of bacteriophage T4. Nature (London) **227:**680–685.
34. **Li, H., H. P. Ko, and J. P. Whitlock, Jr.** 1996. Induction of phosphoglycerate kinase I gene expression by hypoxia. J. Biol. Chem. **271:**21262–21267.
35. **Lillie, J. W., and M. R. Green.** 1989. Transcription activation by the adenovirus E1a protein. Nature (London) **338:**39–44.
36. **Lindebro, M. C., L. Poellinger, and M. L. Whitelaw.** 1995. Protein-protein interaction via PAS domains: role of the PAS domain in positive and negative regulation of the bHLH/PAS dioxin receptor-Arnt transcription factor complex. EMBO J. **14:**3528–3539.
37. **Lucente, D., H. M. Chen, D. Shea, S. N. Samec, M. Rutter, R. Chrast, C. Rossier, A. Buckler, S. E. Antonarakis, and M. K. McCormick.** 1995. Localization of 102 exons to a 2.5 Mb region involved in Down syndrome. Hum Mol. Genet. **4:**1305–1311.
38. **Ma, Q., L. Dong, and J. P. Whitlock, Jr.** 1996. Transcriptional activation by the mouse Ah receptor. J. Biol. Chem. **270:**12697–12703.
39. **Mailly, F., G. Bérubé, R. Harada, P.-L. Mao, S. Phillips, and A. Nepveu.** 1996. The human Cut homeodomain protein can repress gene expression by two distinct mechanisms: active repression and competition for binding site occupancy. Mol. Cell. Biol. **16:**5346–5357.
40. **McGuire, J., P. Coumailleau, M. L. Whitelaw, J. A. Gustafsson, and L. Poellinger.** 1995. The basic helix-loop-helix/PAS factor Sim is associated with hsp90. J. Biol. Chem. **270:**31353–31357.
41. **Moffett, P., M. Duyao, M. Reece, M. K. McCormick, and J. Pelletier.** 1996. Characterization of *msim*, a murine homologue of the *Drosophila sim* transcription factor. Genomics **35:**144–155.
41a. **Moffett, P., and J. Pelletier.** Unpublished data.
42. **Murre, C., G. Bain, M. A. van Dijk, I. Engel, B. A. Furnari, M. E. Massari, J. R. Matthews, M. W. Quong, R. R. Rivera, and M. H. Stuiver.** 1994. Structure and function of helix-loop-helix proteins. Biochim. Biophys. Acta **1218:**129–135.
43. **Nambu, J. R., W. Chen, S. Hu, and S. T. Crews.** 1996. The *Drosophila melanogaster similar* bHLH-PAS gene encodes a protein related to human hypoxia-inducible factor 1α and *Drosophila* single-minded. Gene **172:**249–254.
44. **Nambu, J. R., J. O. Lewis, K. A. Wharton, Jr., and S. T. Crews.** 1991. The *Drosophila single-minded* gene encodes a helix-loop-helix protein that acts as a master regulator of CNS midline development. Cell **67:**1157–1167.
45. **Probst, M. R., C.-M. Fan, M. Tessier-Lavigne, and O. Hankinson.** 1997. Two murine homologs of the Drosophila single-minded protein that interact with the mouse aryl hydrocarbon receptor nuclear translocator protein. J. Biol. Chem. **272:**4451–4457.
46. **Reddy, J. C., and J. D. Licht.** 1996. The WT1 Wilms' tumor suppressor gene: how much do we really know? Biochem. Biophys. Acta **1287:**1–28.
47. **Reisz-Porszasz, S., M. R. Probst, B. N. Fukunaga, and O. Hankinson.** 1994. Identification of functional domains of the aryl hydrocarbon receptor nuclear translocator protein (ARNT). Mol. Cell. Biol. **14:**6075–6086.
48. **Reyes, H., S. Reisz-Porszasz, and O. Hankinson.** 1992. Identification of the Ah receptor nuclear translocator protein (Arnt) as a component of the DNA binding form of the Ah receptor. Science **256:**1193–1195.
49. **Sambrook, J., E. F. Fritsch, and T. Maniatis.** 1989. Molecular cloning: a laboratory manual, 2nd ed. Cold Spring Harbor Laboratory, Cold Spring Harbor, N.Y.
50. **Sanger, F., S. Nicklen, and A. R. Coulson.** 1977. DNA sequencing with chain-terminating inhibitors. Proc. Natl. Acad. Sci. USA **74:**5463–5467.
51. **Sogawa, K., R. Nakano, A. Kobayashi, Y. Kikuchi, N. Ohe, N. Matsushita, and Y. Fujii-Kuriyama.** 1995. Possible function of Ah receptor nuclear translocator (Arnt) homodimer in transcriptional regulation. Proc. Natl. Acad. Sci. USA **92:**1936–1940.
52. **Swanson, H. I., W. K. Chan, and C. A. Bradfield.** 1995. DNA binding specificities and pairing rules of the Ah receptor, ARNT, and SIM protein. J. Biol. Chem. **270:**26292–26302.
53. **Thomas, J. B., S. T. Crews, and C. S. Goodman.** 1988. Molecular genetics of the *single-minded* locus: a gene involved in the development of the *Drosophila* nervous system. Cell **52:**133–141.
54. **Tian, H., S. L. McKnight, and D. W. Russell.** 1997. Endothelial PAS domain protein 1 (EPAS1), transcription factor selectively expressed in endothelial cell. Genes Dev. **11:**72–82.
55. **Voegel, J. J., M. J. S. Heine, C. Zechel, P. Chambon, and H. Gronemeyer.** 1996. TIF2, a 160 kDa transcriptional mediator for the ligand-dependent activation function AF-2 of nuclear receptors. EMBO J. **15:**3667–3675.
56. **Wang, G. L., B.-H. Jiang, E. A. Rue, and G. Semenza.** 1995. Hypoxia-inducible factor 1 is a basic-helix-loop-helix-PAS heterodimer regulated by cellular O_2 tension. Proc. Natl. Acad. Sci. USA **92:**5510–5514.
57. **Whitelaw, M. L., J.-A. Gustafsson, and L. Poellinger.** 1994. Identification of transactivation and repression functions of the dioxin receptor and its basic helix-loop-helix/PAS partner factor Arnt: inducible versus constitutive modes of regulation. Mol. Cell. Biol. **14:**8343–8355.
58. **Wilk, R., I. Weizman, and B.-Z. Shilo.** 1996. *trachealess* encodes a bHLH-PAS protein that is an inducer of tracheal cell fates in *Drosophila*. Genes Dev. **10:**93–102.
59. **Yamaguchi, Y., and T. Tien Kuo.** 1995. Functional analysis of aryl hydrocarbon receptor nuclear translocator interactions with aryl hydrocarbon receptor in the yeast two-hybrid system. Biochem. Pharmacol. **50:**1295–1302.
60. **Yamaki, A., S. Noda, J. Kudoh, N. Shindoh, H. Maeda, S. Minoshima, K. Kawasaki, Y. Shimizu, and N. Shimizu.** 1996. The mammalian *Single-minded* (*Sim*) gene: mouse cDNA structure and diencephalic expression indicate a candidate gene for Down syndrome. Genomics **35:**136–143.
61. **Yao, T., G. Ku, N. Zhou, R. Scully, and D. Livingston.** 1996. The nuclear hormone receptor coactivator SRC-1 is a specific target of p300. Proc. Natl. Acad. Sci. USA **93:**10626–10631.
62. **Zhou, Y.-D., M. Barnard, H. Tian, X. Li, H. Z. Ring, U. Franke, J. Shelton, J. Richardson, D. W. Russell, and S. McKnight.** 1997. Molecular characterization of two mammalian bHLH-PAS domain proteins selectively expressed in the central nervous system. Proc. Natl. Acad. Sci. USA **94:**713–718.